INFORMATION TO USERS

This manuscript has been reproduced from the microfilm master. UMI films the text directly from the original or copy submitted. Thus, some thesis and dissertation copies are in typewriter face, while others may be from any type of computer printer.

The quality of this reproduction is dependent upon the quality of the copy submitted. Broken or indistinct print, colored or poor quality illustrations and photographs, print bleedthrough, substandard margins, and improper alignment can adversely affect reproduction.

In the unlikely event that the author did not send UMI a complete manuscript and there are missing pages, these will be noted. Also, if unauthorized copyright material had to be removed, a note will indicate the deletion.

Oversize materials (e.g., maps, drawings, charts) are reproduced by sectioning the original, beginning at the upper left-hand corner and continuing from left to right in equal sections with small overlaps. Each original is also photographed in one exposure and is included in reduced form at the back of the book.

Photographs included in the original manuscript have been reproduced xerographically in this copy. Higher quality 6" x 9" black and white photographic prints are available for any photographs or illustrations appearing in this copy for an additional charge. Contact UMI directly to order.

UMI

A Bell & Howell Information Company
300 North Zeeb Road, Ann Arbor MI 48106-1346 USA
313/761-4700 800/521-0600

Quantitative analysis of the extracellular glutamate concentration of the Nucleus Accumbens

Katherine Bonter

A Thesis

in

The Department

of

Chemistry and Biochemistry

Presented in Partial Fulfillment of the Requirements

for the Degree of Master of Science at

Concordia University

Montreal, Quebec, Canada

January 1997

ABSTRACT

Quantitative analysis of the extracellular glutamate concentration of the Nucleus Accumbens

Katherine Bonter
Concordia University, 1997

Intracerebral microdialysis was used to sample neurotransmitters from the extracellular fluid of the nucleus accumbens (NAS). Sample concentrations of dopamine and glutamate were assayed using high performance liquid chromatography followed by electrochemical detection. Sample glutamate concentrations decreased and then increased during the first ten to twelve hours following probe implantation. After stabilization sample glutamate and dopamine concentrations were estimated at a range of flow rates (0.25 µl/m, 0.5 µl/m, 1.0 µl/m, 2.0 µl/m); dopamine and glutamate concentrations varied inversely with the rate of perfusion. Estimates of the normal NAS extracellular glutamate and dopamine concentrations could not be obtained from these data using the "extrapolation to zero flow" method because there was no evidence of asymptotic yield within the range of flow rates that could be tested. An estimate of the normal NAS extracellular glutamate concentration (4.0 ± 0.8) was obtained using the no-net-flux method. The no-net-flux estimate was not significantly affected by an increase in the local depletion of dopamine and other small molecules caused by doubling the perfusate flow rate. The estimated extracellular glutamate concentration was 3.8 ± 0.8 µM at a flow rate of 0.5 µl/m and 4.25 ± 0.9 µM at a flow rate of 1.0 µl/min. These concentrations are not significantly different, suggesting that this increase in local depletion did not influence the activity of glutamate releasing cells in the tissue adjacent to the probe. Changes in dialysis sample dopamine concentration were determined during the extraction of NAS glutamate or the delivery of glutamate to the NAS. No significant changes in the sample dopamine concentration were

associated with the perfusion of a range of glutamate concentrations surrounding the estimated NAS extracellular glutamate concentration.

Acknowledgments

My sincerest thanks to all of those who helped me along the way. Your support, advice, and direction were greatly appreciated.

Index of Figures

Chapter One

General Introduction

1.0 Introduction to Microdialysis

Cellular interactions essential to central nervous system (CNS) function depend on biochemical signaling between neurons. This biochemical signaling influences the biochemical composition of the brain extracellular fluid and can be monitored using techniques that sample the extracellular fluid. One such technique is intracerebral microdialysis which can be used in correlating extracellular neurochemical changes with changes in the neurophysiology or behaviour of conscious animals.

Brain microdialysis involves implanting a probe into a brain region of interest. The active part of a microdialysis probe is a length of cylindrical dialysis membrane which is perfused with a solution (the perfusate) of an ionic composition and pH similar to that of the brain extracellular fluid. Molecules smaller than the pores in the membrane diffuse between the perfusate and the extracellular fluid. Small molecules in the extracellular fluid at a concentration greater than that of the perfusate diffuse into the perfusate and small molecules in the perfusate at a concentration greater than that of the extracellular fluid are delivered to the tissue. Thus microdialysis can be used to deliver or sample neurochemicals to or from the extracellular fluid of a particular brain region.

1.1 Theoretical description of dialysis

Dialysis is driven by the random motion of molecules which leads to their net diffusion through a semi-permeable membrane. This diffusion is described by Fick's law; which states that the flux (f)—the rate of diffusion of a molecule across a dialysis membrane—is proportional to the concentration gradient (ΔC; moles/l) of that molecule across the membrane. The ΔC's across the membrane influence the rates at which

molecules diffuse through the membrane, determine the direction of diffusion, and determine the net diffusion across the membrane required for equilibrium to occur. Fick's equation describes the absolute relationship between flux and ΔC.

$$f = D \cdot \phi \cdot \Delta C$$

This equation contains two constants: the diffusion coefficient (D; length^2/time) and the membrane porosity (ϕ; time/length^2). The diffusion coefficient of a given molecule depends on the total resistance to the diffusion of the molecule through the media that contain the concentration gradient. Membrane porosity determines which molecules can diffuse through the membrane. Important determinants of diffusion across the dialysis membrane of a microdialysis probe are: the selectivity of the dialysis membrane, the distance diffused by the analyte, the resistance to diffusion encountered, and the magnitude of the concentration gradient across the membrane. These determinants can be influenced by physical characteristics of the microdialysis probe and perfusate as well as physiological characteristics of the tissue external to the dialysis probe.

1.1.1 Pore size of dialysis membrane

The size of the pores in the dialysis membrane determine the selectivity of diffusion across the dialysis membrane and the maximal rate of dialysis; pore size limits the number of molecules that can pass simultaneously though each pore. Larger pores offer less resistance to diffusion and will allow the passage of more molecules simultaneously; thus a higher rate of dialysis is possible when other factors are not limiting.

1.1.2 Length of dialysis membrane

The effect of changes in the length of dialysis membrane on the extraction of dopamine (DA), dihydroxyphenyl acetic acid (DOPAC), homovanillic acid (HVA), 5-hydroxyindoleacetic acid (5-HIAA), glutamate, aspartate, and γ-aminobutyric acid (GABA) has been investigated. It has been shown that the longer the membrane the greater the extraction of a given compound (Johnson, and Justice, 1983; Tossman, and

Ungerstedt, 1986; Lindefors, *et al.*, 1989). The portion of the external analyte extracted is greater with longer probes because of an increase in the surface area of exposed membrane and an increase in the time allowed for equilibration between the perfusate and the extracellular fluid. The relationship between extraction and dialysis membrane length is linear for membrane lengths between 1-20 mm long (Jacobson, *et al.*, 1985)

1.1.3 Perfusate Composition

The perfusate commonly used for intracerebral microdialysis has an ionic composition similar to that of the brain extracellular fluid. The perfusate may also contain ascorbic acid and glucose at concentrations equal to the normal brain extracellular concentration. Perfusate, with a physiological pH, is perfused at a low pressure to eliminate physical causes of diffusion other than the concentration gradients across the dialysis membrane. If the analyte concentration of the perfusate is different from the extracellular concentration then perfusate flow imposes a ΔC of analyte across the membrane. The magnitude of this gradient and therefore the rate of analyte dialysis is determined in part by the analyte concentration of the perfusate.

1.1.4 Perfusion flow rate

An increase in the rate of perfusion causes a decrease in the net time that incoming perfusate is exposed to the dialysis membrane; less time is allowed for equilibration across the dialysis membrane increasing the net size of the ΔC's across the membrane and the rates of dialysis. As flow rate is decreased more time is allowed for equilibration, decreasing the net size of the ΔC's across the membrane and reducing the rates of dialysis. An increase in the rate of analyte dialysis leads to an increase in the absolute quantity of analyte collected per sample and a decrease in the analyte concentration of each sample. The relationships between perfusate flow rate and the rates of *in vitro* and *in vivo* extraction of DOPAC, HIAA, HVA, GABA and glutamate have been demonstrated experimentally (Zetterstrom, *et al.*, 1983; Ungerstedt, 1984; Wages, *et al.*, 1986).

1.2 Physiology of neuronal tissue

1.2.1 Neurotransmission

Neurons respond to specific neurochemicals present in the synaptic or extracellular fluid. These external neurochemical signals can be transduced by neurons into bioelectric signals (action potentials) that are transmitted to other neurons in distal regions of the brain. The cell body of a neuron contains the nucleus and extends: (i)processes that receive inputs from other neurons (the dendrites) and (ii)a process that transmits output to other neurons (the axon). The axon conducts bioelectric signals from the cell body to the terminal region. The terminal of the axon is specialized for the exocytotic release of neurotransmitter in response to an action potential. The terminal membrane forms a synapse with the plasma membrane of the opposing neuron (postsynaptic membrane). The synapse is the site of neurochemical transmission through the extracellular space.

The capacity of a neuron to transmit and transduce bioelectric signals depends on the electrochemical properties of the plasma membrane. Plasma membrane proteins actively maintain different ion concentrations on either side of the plasma membrane, resulting in a transmembrane electrochemical potential. A change in the activity of these proteins can cause a change in the transmembrane electrochemical potential—depolarization or hyperpolarization of the membrane.

An action potential is a brief depolarization and repolarization of a region of the axonal membrane that propagates along the axon as an electrical wave. An action potential is initiated if the axon hillock (region between the cell body and axon) is depolarized beyond a threshold potential. This threshold depolarization of the axon hillock occurs due to the summation of depolarizing biochemical inputs to the cell body and dendrites. The wave of electrical activity that passes along the axon during an action potential results from the sequential opening and closing of voltage-sensitive ion channels

present in the axon plasma membrane and the passage of ions through these channels according to the electrochemical gradients across the axonal membrane.

Depolarization during an action potential occurs due to sodium influx through voltage-sensitive sodium channels; the recovery of the membrane potential back to the resting potential and hyperpolarization of the membrane, depends on potassium ion efflux through voltage-sensitive potassium channels. This potassium flux is activated by the depolarization phase of the action potential. Depolarization of the terminal region of the axon activates voltage-sensitive calcium channels that allow calcium ion influx. Calcium influx initiates the fusion of exocytotic vesicles, containing neurotransmitter, to the presynaptic membrane and causes the exocytotic release of neurotransmitter into the synapse.

1.2.2 Neuroglia

Neuroglia are the interstitial cells of nervous tissue. These cells have essential supportive and metabolic roles in neuronal function (Hansson, and Ronnback, 1995). Glial cells differ from neurons in that they do not make synaptic contacts or have the specialized morphology of neurons. Glial cells make physical connections with neurons via gap junctions and desmosomes. These connections allow for direct communication between neurons and glia. Glial cell activity is critical to the functioning of neurons and contributes in various ways to the composition of the extracellular fluid in the vicinity of the probe. Glial cells: pack and insulate the neuronal component of CNS, aid in the repair of damaged neurons, produce neuronal substrates and metabolize neurotransmitters, regulate local pH levels and ionic balance, and transport compounds across the blood brain barrier.

1.3 The nucleus accumbens

The microdialysis data presented in this thesis were obtained using probes implanted into the nucleus accumbens (NAS) of the rat brain (Figure1). The NAS is the

rostro-ventral portion of the striatum; it is associated with the neural processes that influence motivation and emotion (Wise, *et al.*, 1989; Schultz, *et al.*, 1992).

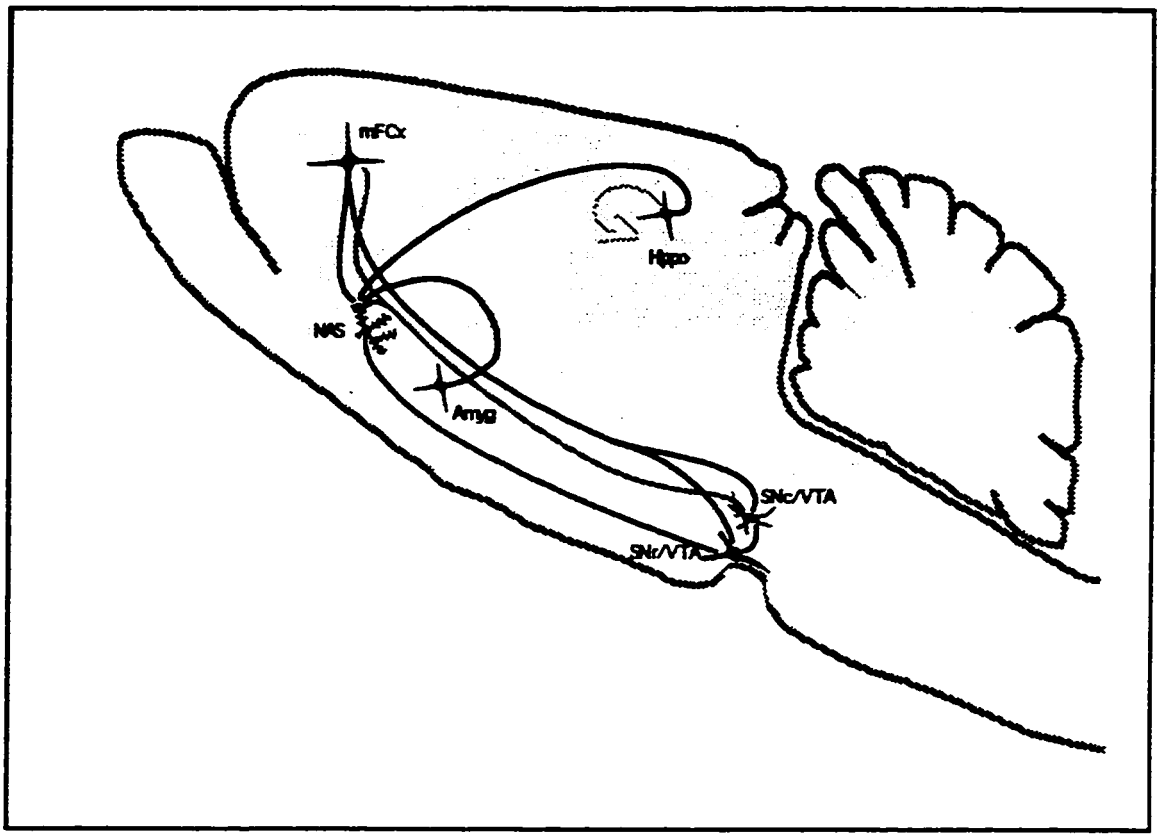

Figure 1: *Rat brain sagital section.* Diagram illustrating relevant central neuronal structures and the major synaptic relationships between glutamatergic and dopaminergic projections to the nucleus accumbens (NAS). The star shapes represent cell bodies; the lines represent axons. Lines denote: glutamatergic projections from the hippocampus (Hippo), prefrontal cortex (PFC) and amygdala (Amyg), dopaminergic projections from the ventral tegmental area (VTA) to the nucleus accumbens (NAS) and prefrontal cortex (PFC), and GABAergic projections from the VTA to the NAS.

Dialysis samples were obtained from probes implanted into the NAS and subsequently assayed for dopamine and glutamate. In order to interpret changes in the sample concentrations of dopamine and glutamate it is important to consider the cellular composition of the NAS, the sources of NAS extracellular dopamine and glutamate, and the glial and neuronal physiology that modulate the NAS extracellular concentrations of dopamine and glutamate.

The NAS contains intrinsic neurons that project to other brain regions. In addition the NAS contains two or more types of interneurons (neurons that reside completely within the NAS), and terminals of efferent neurons (neurons that project to the NAS from other brain regions and synapse on intrinsic cell bodies). The primary efferent projections are a dopaminergic projection from the ventral tegmental area (Fallon, J.H. and Moore, R.Y., 1978; Fallon, J.H., 1988) , and glutamatergic projections from the prefrontal cortex (Sesack, S.R. et al., 1989), amygdala (Fuller, T.A. et al., 1987; Kita, H. and Kitai, S.T., 1990) and hippocampus (Totterdell, S. and Smith, A.D., 1989). These glutamatergic and dopaminergic inputs converge on dendrites and cells bodies within the NAS (Figure 1).

Electrophysiological techniques have been used to study the response of NAS neurons to the activation of glutamatergic and dopaminergic inputs. Electrical stimulation of projections from the hippocampus, amygdala, and prefrontal cortex excite NAS cell bodies. This excitation is influenced by concurrent stimulation of dopaminergic efferents from the ventral tegmental area, and application of dopaminergic drugs to the NAS (Yang, and Mogenson, 1984; Yang, and Mogenson, 1986; Yim, and Mogenson, 1986; O'Donnell, and Grace, 1993; O'Donnell, and Grace, 1994). Responses elicited by the stimulation of the hippocampus, amygdala, and prefrontal cortex summate on individual NAS cells and hippocampal input is necessary for activation of NAS cells via stimulation of cortical or amygdaloid inputs (O'Donnell, and Grace, 1995). Furthermore, the behavioural effects of NAS dopamine can be influenced by infusing glutamatergic

drugs into the NAS and behaviours mediated by NAS glutamate can be influenced by infusing dopaminergic drugs into the NAS (Pulvirenti, *et al.*, 1991; Kelley and Throne, 1992; Wu, *et al.*, 1993; Burns, *et al.*, 1994; Hooks, and Kalivas, 1994). It has also been shown using microdialysis that NAS extracellular dopamine concentration can be modulated by infusing glutamate or glutamatergic drugs into the NAS (Imperato *et al.*, 1990; Imperato, *et al.*, 1990; Youngren, *et al.*, 1993; Bianchi, *et al.*, 1994; Pap, and Bradberry, 1995; Taber, and Fibiger, 1995) . Together these data demonstrate that the activity of NAS dopamine releasing cells and NAS extracellular dopamine concentration can be influenced glutamate releasing cells and nerve terminals in the NAS.

1.4 Effect of perfusate composition on tissue physiology

The extraction of molecules from the extracellular fluid by dialysis can lead to depletion of molecules from the tissue adjacent to the probe. Depletion of neurotransmitters, ions, or other endogenous compounds may lead to changes in the activity of cells in the tissue proximal to the probe. Because the levels of some neurotransmitters and metabolites are under local regulatory control, it is important to assess the consequences of this extraction on the subsequent levels of other neurotransmitters or metabolites.

The ion gradients across the plasma membranes of neurons and glia are essential for chemical neurotransmission (Section 1.2.1 pg. 4). Transmembrane ion gradients also provide the driving force for the uptake of extracellular neurotransmitter following exocytotic release, the process by which dopaminergic neurotransmission and glutamatergic neurotransmission are terminated. Microdialysis sampling can alter extracellular ion concentrations in the tissue adjacent to the probe. Alterations in ion concentration may influence the exocytotic release of neurotransmitter, the reuptake of neurotransmitter, and the basal responsiveness of neurons.

The extracellular dopamine concentration of the striatum, as inferred from microdialysis data, is sensitive to changes in extracellular calcium, magnesium, sodium, and potassium concentrations. The extracellular concentrations of these ions can be perturbed if the ionicity of the perfusate is different from that of the extracellular fluid. For example, Ringer's solution mimics the ionic composition of plasma; the potassium and calcium concentrations of Ringer's solution are twice the brain extracellular concentrations, and the magnesium concentration of Ringer's solution is one half the brain extracellular concentration. During the perfusion of Ringer's solution basal striatal dopamine levels are 175% greater than basal levels during perfusion of a solution with the same ionicity as the extracellular fluid (Moghaddam, B. and Bunney, B.S., 1989). Increases in the perfusate concentration of potassium, sodium or calcium also increase extracellular levels of striatal dopamine (Moghaddam and Bunney, 1989; Westerink *et al.*, 1989; Osborne *et al.*, 1991). These findings demonstrate the capacity of the ionic composition of the perfusate to affect the extracellular neurotransmitter concentrations.

1.5 Relevance of dialysis sample measures to neurotransmission

The aim of intracerebral microdialysis studies is to estimate changes in extracellular concentration that reflect the activity of cells in the tissue adjacent to the microdialysis probe. A variety of neuroactive compounds are released into or removed from the extracellular fluid by both neurons and glia and some of these compounds can be collected in dialysis samples and quantified. Dialysis sample composition can be related to the activity of neurons or glia only if the physiological factors that influence and determine the extracellular concentrations of compounds of interest have been defined.

Neurotransmission depends on the exocytotic release of neurotransmitter from nerve terminals in response to calcium influx initiated by depolarization of terminal membranes. Based on this concept of neurotransmission criteria for the characterization

of dialysis sample neurotransmitter content have been proposed: (i) dialysate neurotransmitter concentrations should decrease if sodium influx is antagonized by perfusing tetrodotoxin (TTX—a toxin which blocks voltage dependent sodium channels), (ii) dialysate neurotransmitter concentrations should decrease if calcium influx through voltage dependent calcium channels is antagonized either by depleting calcium or by perfusing calcium antagonists such as Mg^{2+} or Cd^{2+}.

Microdialysis extraction disturbs the extracellular concentrations of compounds that diffuse across the dialysis membrane. The present experiments were designed to estimate the "undisturbed" extracellular glutamate concentration of the NAS and to investigate the influence of dialysis induced disturbances on NAS extracellular concentrations of glutamate and dopamine. To this end, an assay for glutamate was established and used to characterize the stabilization of sample glutamate concentrations following probe implantation.

The effects of probe implantation on the activity of NAS cells and the stabilization of dialysis sample glutamate and dopamine concentrations following probe implantation are characterized in Chapter Two. Other data presented in Chapter Two characterize the variability inherent to the analysis of the glutamate concentration of NAS dialysis samples. Chapter Three describes the estimation of the NAS extracellular glutamate concentration and the effects of dialysis extraction on levels of glutamate and dopamine in dialysis samples obtained from probes implanted in the NAS.

Chapter Two

Characterization of Methods

2.0 Introduction

2.0.1 Probe implantation

Probe implantation causes acute tissue damage and alters the extracellular environment of cells near the probe (Benveniste, 1989; Major, *et al.*, 1990; Shuaib *et al.*, 1990; Kurosawa et al., 1991; Fumero, *et al.*, 1994). The tissue damage caused by probe implantation is associated with elevated dialysis sample dopamine concentration and is assumed to influence extracellular levels of other neurotransmitters . It has been suggested that this elevation occurs because dopamine leaks from cells damaged during probe implantation (Westerink and DeVries, 1988; Camp, and Robinson, 1992; Robinson and Camp, 1992; Campbell *et al.*, 1993). Because of this possibility it is important to determine when sample neurotransmitter levels reflect the normal functioning of cells in the tissue next to the dialysis membrane. To this end investigators have studied the dependence of sample neurotransmitter content on the propagation of action potentials and the exocytosis of neurotransmitter from nerve terminals.

2.0.2 Dependence of dialysis sample dopamine content on action potential propagation and exocytosis

Up to four hours after implantation, as much as 90% of the dopamine signal monitored does not depend on action potential propagation, nerve terminal depolarization, and exocytotic neurotransmitter release. Tetrodotoxin inhibits action potential propagation by blocking sodium flux through voltage dependent sodium channels. Tetrodotoxin perfused into striatum immediately following probe implantation decreases the sample dopamine concentration by 10%, indicating that only 10% of the dopamine collected is released into the extracellular fluid by depolarization induced

exocytosis from nerve terminals. The sensitivity of sample dopamine concentration to TTX increases with time following implantation. Maximum sensitivity is attained approximately 4 to 6 hours following probe implantation. Perfusing 1 or 10 μM TTX, 4 to 6 hours following implantation, causes a 90 to 95% decrease in sample dopamine concentration (Westerink and DeVries, 1988; Drew *et al.*, 1989). This maximum sensitivity to TTX has also been observed 24 and 48 hours following probe implantation (Westerink and DeVries,, 1988). These findings indicate that the dopamine signal monitored 5 and 48 hours after probe implantation is a reliable measure of dopaminergic neurotransmission.

Another index of normal neuronal function derives from the calcium dependence of synaptic transmission. Flux of calcium into the nerve terminal occurs following transmission of an axon potential to the terminal region. This calcium influx depolarizes the terminal membrane and initiates exocytotic neurotransmitter release. Calcium influx into the terminal can be reduced by perfusing a calcium free perfusate and depleting extracellular calcium, or by perfusing a calcium antagonist. These treatments cause a 70% to 90% decrease in sample dopamine concentration, 5, 24 and 48 hours following probe implantation (Westerink and DeVries, 1988). Like the effects of TTX, these findings demonstrate that up to 90% of the dopamine collected in dialysis samples, 5 to 48 hours post implantation, is released from neurons into the extracellular fluid by depolarization induced exocytosis. The partial insensitivity of dopamine to treatment with TTX or calcium antagonists (10% to 20%) may be due to an incomplete block of sodium or calcium flux by these treatments or due to a physiological dopamine release that is independent of membrane depolarization and exocytosis.

The effects of TTX and calcium antagonism on microdialysis measures of striatal GABA and glutamate concentrations have also been investigated. These manipulations have very little effect on basal sample GABA or glutamate obtained from the striatum at any time following probe implantation (Westerink and DeVries, 1988; Drew *et al.*, 1989).

Based on these findings it has been suggested that basal levels of extracellular glutamate and GABA, monitored by microdialysis, may be determined by factors other than depolarization induced exocytosis from nerve terminals.

2.0.3 Physiological changes that occur during microdialysis

The activity of glial cells is influenced by many things including tissue damage or the presence of a foreign object (Hamberger *et al.*, 1983; Hamberger and Nystrom, 1984; Benveniste, 1989; Shuaib *et al.*, 1990; Robinson and Camp, 1991; Robinson and Camp, 1992). These insults initiate the swelling of resting glial cells (nuclei and cytoplasm) and glial cell proliferation. Following proliferation, resting glial cells are transformed into reactive astroglia that form a scar in the injured region (Kitamura, 1980). Changes in glial activity occur up to 48 hours following probe implantation. Reactive-glia, unlike resting-glia, release eicosanoids and cytokines into the extracellular fluid and variations in dialysis sample concentrations of these compounds have been observed up to 48 hours after probe implantation. Eicosanoids and cytokines can influence neuronal activity in a variety of ways (Yergey and Heyes, 1990; Woodroofe *et al.*, 1991). Furthermore, changes in glial activity can influence extracellular levels of glutamate, GABA, and dopamine (Paulsen and Fonnum, 1989; Wang *et al.*, 1994) and resting glia have a direct role in the uptake and metabolism of neurotransmitter pools of glutamate and GABA (Fonnum, 1993; Nicholls, 1993; Hansson and Ronnback, 1995; Laake *et al.*, 1995). Hence the tissue damage that accompanies probe implantation leads to changes in the activity of glial cells that can influence the activity of both dopaminergic and glutamatergic neurons in the tissue next to the dialysis membrane.

2.0.4 Repeated measures

Repeated analyses of identical samples were done to determine the variability inherent to the glutamate assay. Sample preparation and injection were automated; samples were preloaded into an auto-injector and remained at room temperature for up to nine hours prior to sample preparation and analysis. This characterization was important for subsequent data analysis and interpretation because it enabled identification of variations in sample glutamate concentration that reflected changes in extracellular glutamate concentration.

2.1 Methods

2.1.1 Animals and surgery

Twenty-five male Long-Evans rats (Charles River, Quebec) weighing 300-350 grams at the time of surgery were used. Prior to experiments, the animals were housed under controlled environmental conditions (temperature 22 °C; humidity 60-65%; light 6 a.m. to 7 p.m., dark 7 p.m. to 6 a.m.). Food and water were available *ad libitum*.

Prior to surgery the rats were anesthetized with sodium pentobarbital (65 mg/kg inter peritoneal) and mounted onto a conventional stereotaxic frame. Surgery was performed with the incisor bar 5 mm above the intra-aural line. The skull surface was exposed and a hole was drilled into the scull at a point 3.4 mm anterior to bregma and 2.4 mm lateral to bregma. The dura in the centre of the hole was penetrated with a needle. Following this preparation a stainless steel 20-gauge guide cannula was lowered at a 10° angle from the midline through the brain (4.3 ventral), terminating in the dorsal part of the striatum, immediately above the NAS. The animals were allowed 7 days recovery time prior to probe implantation and microdialysis.

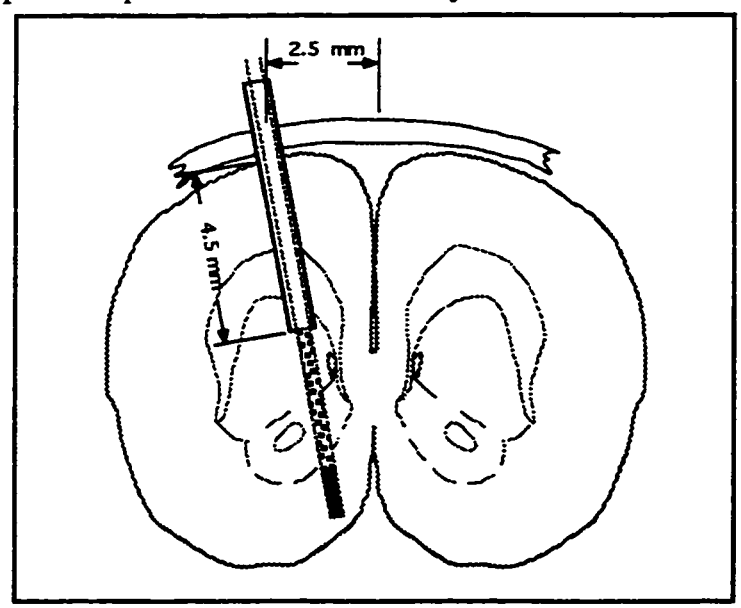

Figure 2: *Cannula Placement: cross section of brain illustrating a probe implanted into the NAS*

2.1.2 Microdialysis

Probe construction

Microdialysis probes were constructed according to the method of Johnston and Justice (1983). Two lengths of silica tubing (Polymicro Technologies Inc., inner diameter, 50 μm; outer diameter, 150 μm), were inserted into a 5 mm segment of cellulose dialysis membrane tubing (Spectrum, inner diameter, 215 μm; outer diameter, 251 μm; molecular weight cut off 6 000 Da). The silica inlet extended 4 mm into the dialysis membrane; the silica outlet extended 2 mm into the dialysis membrane. The open ends of the dialysis tube were sealed with polyamide resin (All-Tech, USA). Resin was also applied to the top 2 mm of the dialysis membrane to inactivate this part of the membrane and to fuse the silica tubes together (Figure 3). This preparation was allowed to dry for at least 24 hours before use. The silica tubes extending from each probe were protected by inserting them into polyethylene tubing (PE 20) which was also fixed to the silica tubing with polyamide resin.

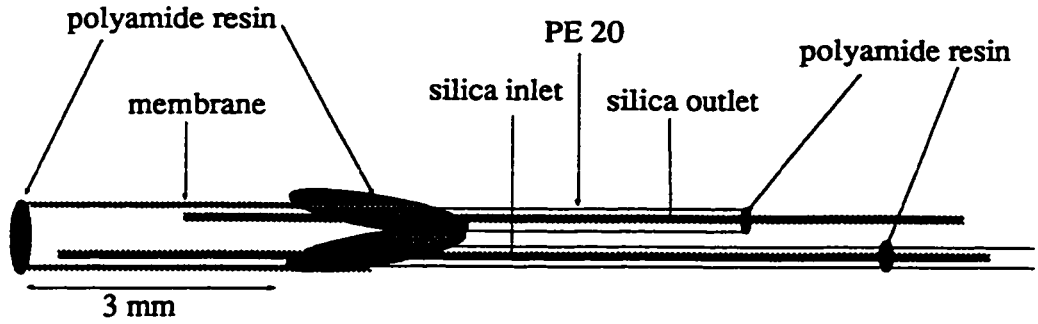

Figure 3: *Cross section of microdialysis probe.*

The open end of the polyethylene tubing containing the inlet silica was later attached to a fluid swivel which was attached to a syringe pump (Razel, model A-99 M). This arrangement enabled free movement of the probe parts that extended from the scull and the collection of dialysis samples from conscious animals.

Sample collection

Samples were collected into polypropylene vials and frozen immediately on dry ice. Samples were stored at -70°C and analyzed at a later date.

Probe implantation

Probes were flushed with perfusate for 24 hours prior to implantation. The perfusate or artificial cerebral spinal fluid (aCSF) was composed of 145 mM sodium chloride, 2.8 mM potassium chloride, 1.2 mM magnesium chloride, 1.2 mM calcium chloride, 0.25 mM ascorbic acid, and 5.4 mM D-glucose (Fisher Scientific, Canada) adjusted to a pH of 7.2-7.4 with sodium hydroxide (Fisher Scientific, Canada).

Each probe was designed to extend 3 mm beyond the tip of the guide cannula; when a probe was passed through the guide cannula a 3 mm segment of dialysis membrane was implanted into the NAS. Six days following surgery the animals were moved from their home cages to the experimental cages and allowed to habituate to the new environment for 24 hours prior to probe implantation. After the probes were implanted the animals remained in these cages until the end of the microdialysis experiment.

2.1.3 Intracardiac perfusion and histology

At the end of the experiment each animal was given an anesthetic dose of sodium pentobarbital. The brains were prepared for slicing by intercardiac perfusion of saline followed by 10% formalin. Following perfusion, each brain was removed from the scull and stored in formalin. At a later date the brains were frozen and 40 μm coronal sections were sliced for verification of the probe placement. All data reported were collected from probes implanted in the NAS.

2.1.4 Sample Analysis

Glutamate Analysis

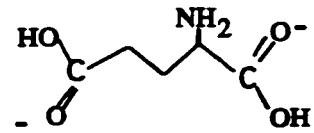

Samples were derivatized with o-phthalaldehyde (OPA) and the contents of each sample separated by reverse-phase high performance liquid chromatography (HPLC). A C_{18} hypersil ODS (octyldecylsiloxane) column was used (5 µm particles, 15 cm x 4.6 cm, Supelco, Canada). The mobile phase contained 0.1 M phosphate buffer, pH 6.2 with 30% methanol and was pumped at a flow rate of 1.0 ml/min by a Waters 510 HPLC pump (Waters, Canada). The retention times and peak widths of the glutamate peaks were consistent between analyses of dialysis samples and amino acid standards. This observation indicates that unidentified compounds in the dialysis sample did not interfere with the analysis of glutamate (Figure 4).

Amino acids were derivatized with OPA in the presence of an alkyl thiol (ß-mercaptoethanol) prior to injection on to the column (Donzanti, and Yamamoto, 1988); (Figure 5). The stock solution of derivatizing reagent was prepared by dissolving 27 mg of OPA in 1 ml of 100% methanol (HPLC grade, Fisher Scientific, Canada). When the OPA was well dissolved, 9 ml of 0.05 M sodium tetraborate (pH 9.4) and 20 µl ß-mercaptoethanol (BME); (Sigma-Aldrich, Canada) were added. This solution was stirred and stored at +4 °C. The stock solution remained active for 3 to 4 days. Each day a working solution—the derivatizing reagent—was made by diluting the stock solution 1:3 with sodium tetraborate buffer (0.05 M).

Chromatogram A

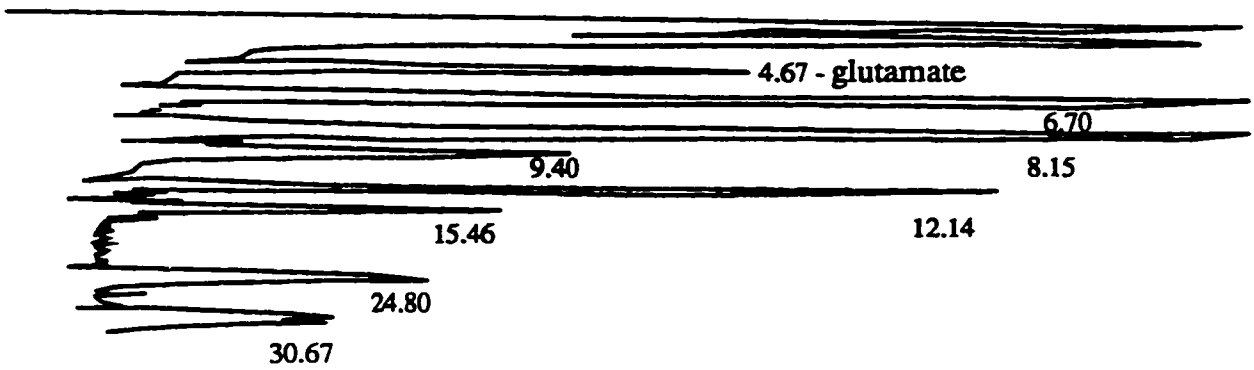

Chromatogram B

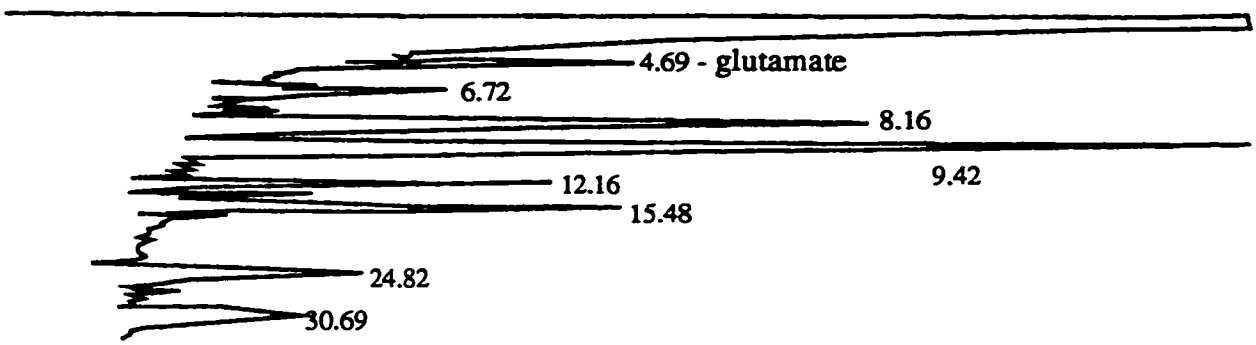

Figure 4: *Sample Chromatograms: amino acid analysis.* Chromatogram A—analysis of 10 µl of a 3 µM amino acid standard. Retention times are expressed in minutes: glutamate-4,67, serine-6.70, arginine-8.15, taurine-9.40, asparagine-12.14, glycine-15.46, glutamine-12.14, alanine-24.80, GABA-30.67. Chromatogram B—analysis of 10 µl of a dialysis sample collected from rat NAS. Retention times are expressed in minutes: glutamate-4,69, serine-6.72, arginine-8.16, taurine-9.42, asparagine-12.16, glycine-15.48, glutamine-12.16, alanine-24.82, GABA-30.69.

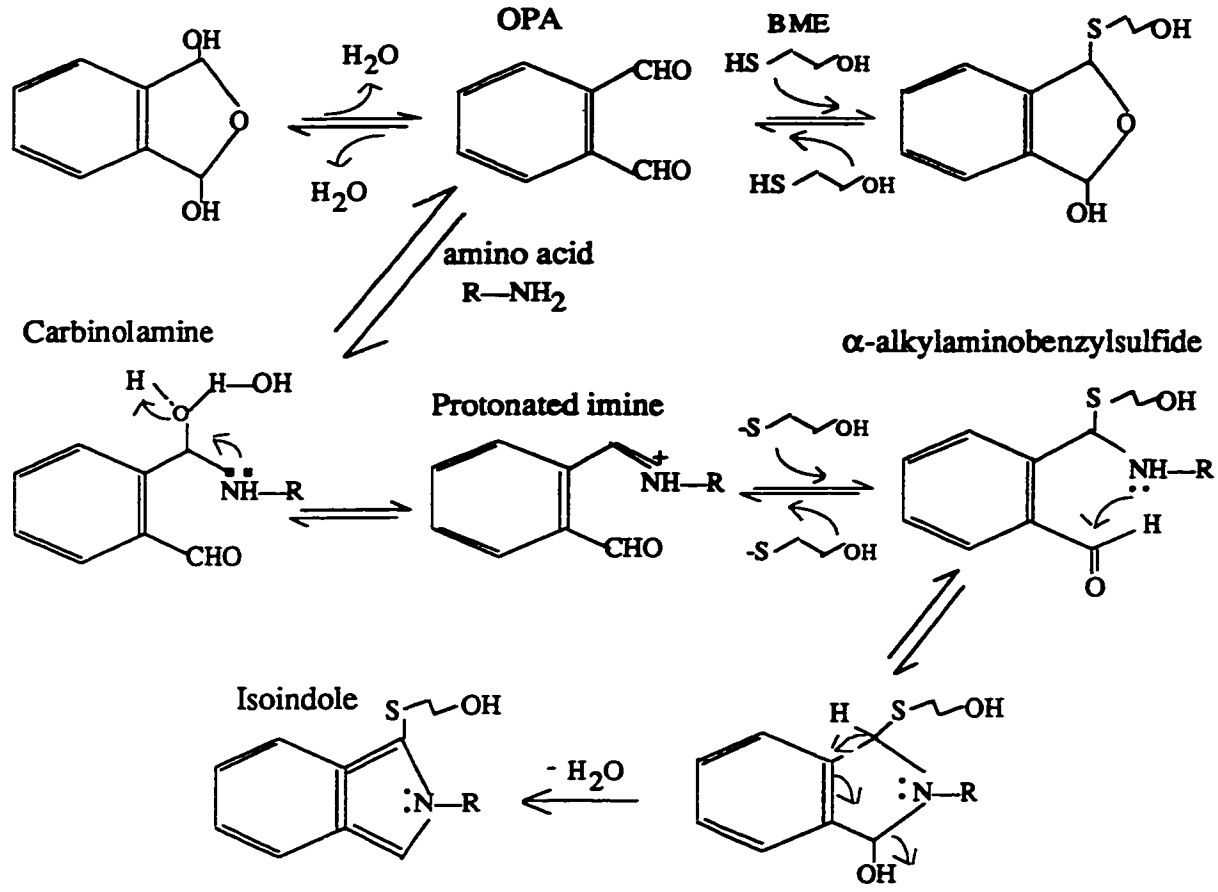

Figure 5: *Amino acid derivatization.* Proposed mechanism of OPA condensation with a thiol (BME) and a primary amine (amino acid); (Sternson, L.A. et al., 1985).

The amino acid content of each derivatized sample was quantified *via* electrochemical detection of the oxidation of OPA-amino acid derivatives at a working electrode delivering a +600 mV potential relative to the reference electrode (constructed of a proprietary material: ESA Inc., USA); (Figure 5). The peak potential range for the oxidation of OPA-amino acid derivatives is from 730–798 mV vs. Ag/AgCl. Compared to methylhydroquinone (n=2) the ratio of the peak currents is 0.85, suggesting a two electron process; however, a mechanism for the oxidation reactions of these isoindole derivatives has not been proposed (Allison, *et al.*, 1984).

The sensitivity of the detector (ESA Coulochem II, USA) was 100 nA (per volt output). The response of the detector was linear in the range of glutamate concentrations analyzed (Figure 6). The detection limit of the glutamate assay (1.6e-6 M) and the sensitivity of the glutamate assay (4.2e+12 area/M) were calculated from a linear regression of these calibration data (appendix 1).

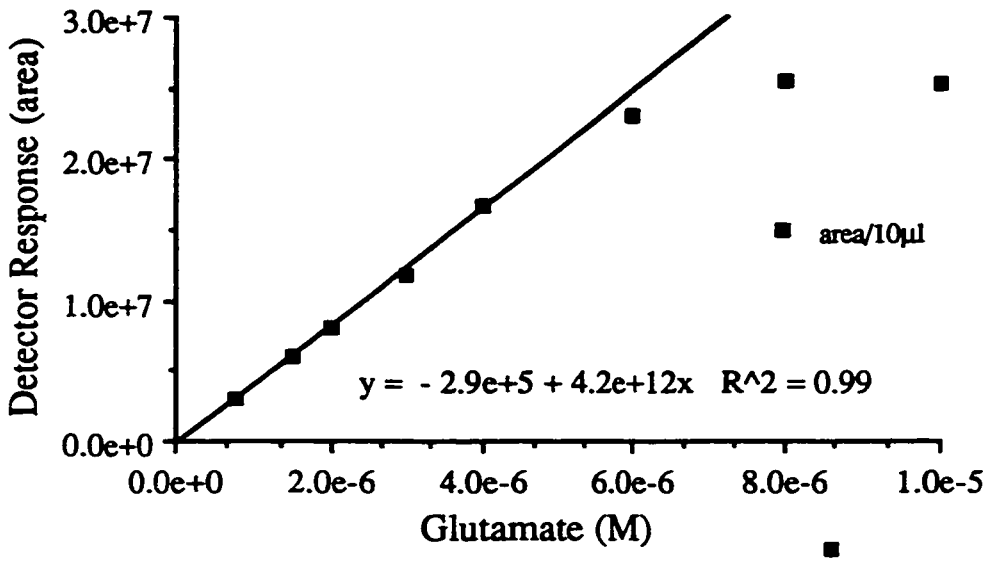

Figure 6: *Detector response curve: oxidation of OPA–glutamate derivatives at +600mV (sensitivity 100 nA/1 Volt).*

Sample preparation and sample injection were automated (Thermoseparation Products, Spectra System AS3500). Vials containing 10 µl of dialysis sample were prepared manually and loaded into the auto-injector. If the volume of the collected sample was less than 10 µl, a volume of aCSF was added to the sample to give a final volume of 10 µl. Similarly, if the concentration of the sample was greater than 5 µM, the sample was diluted with aCSF and 10 µl aliquots of the diluted sample were injected. Delivery of 15 µl of OPA working solution to the 10 µl sample, mixing, and sample injection were automated. Twenty microlitres (of the 25 µl derivatized sample) were injected on to the column *via* a 20 µl Rheodyne injection loop.

Dopamine and DOPAC Analysis

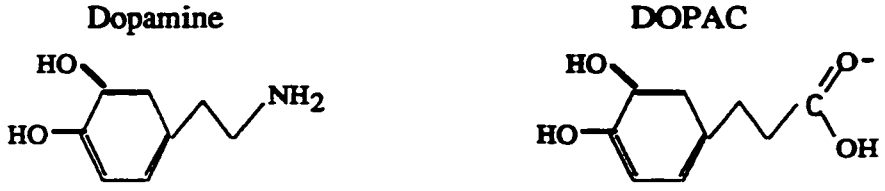

High performance liquid chromatography was used to separate the components of each dialysis sample. A 15 cm X 4.6 mm column with octyldecylsiloxane (C18) surface chemistry (sil ODS/2, 5 μm: Chromatography Sciences, Quebec) was used with the following mobile phase; 0.06M NaH_2PO_4, 0.03 M citric acid, 7.98×10^{-5} sodium dodecyl sulfate SDS, 9.94×10^{-5} ethylenediaminetetraacetic acid (EDTA) in 25% methanol. Mobile phase was recycled and pumped through the system by a ESA pump (model 580) flow rate of 1.2 ml/min. Samples were injected on to the column *via* a Rheodyne injection valve with a 20 μl sample loop.

Dopamine and DOPAC were quantified by electrochemical detection (Kotake, C. et al., 1985). An ESA Coulochem II Detector, Model 211, was used with the electrodes set at the following potentials: +340 mV, oxidizing electrode; and -300 mV, reducing electrode. Dopamine quinone was detected at the reducing electrode (electrode 2, -300 mV) (figure 7); dopamine was converted to dopamine quinone at the first electrode and the reduction of dopamine quinone was measured at the second electrode. DOPAC was detected at the oxidizing electrode (electrode 1, +340 mV) (Figure 8). Because the concentration of dopamine in the dialysate is typically 10^2 less than that of DOPAC, the sensitivity of the reducing electrode (260 mV) was set at 10 nA (per volt output); (Figure 9) and the sensitivity of the oxidizing (+340 mV); (Figure 10) electrode at 500 nA (per volt output).

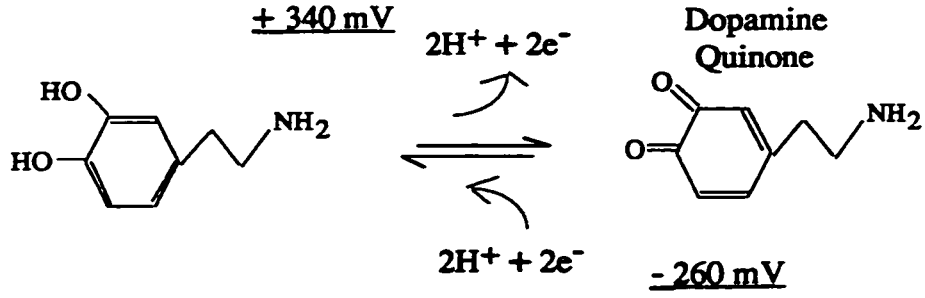

Figure 7: Oxidation of dopamine and reduction of dopamine quinone.(ESA, I., 1988)

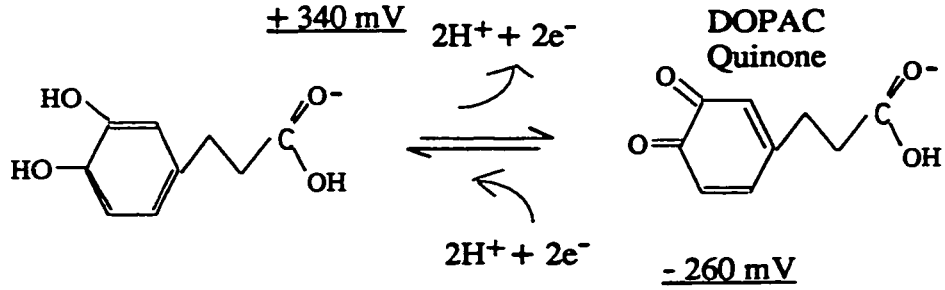

Figure 8: Oxidation of DOPAC and reduction of DOPAC quinone (ESA, I., 1988).

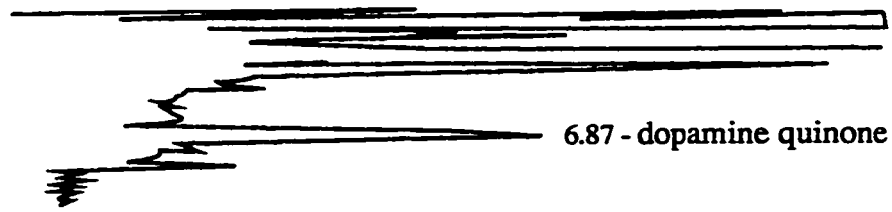

Figure 9: *Sample Chromatogram*: reduction of dopamine quinone (retention time 6.87 min.) in 20 µl of a dialysis sample collected from the rat NAS.

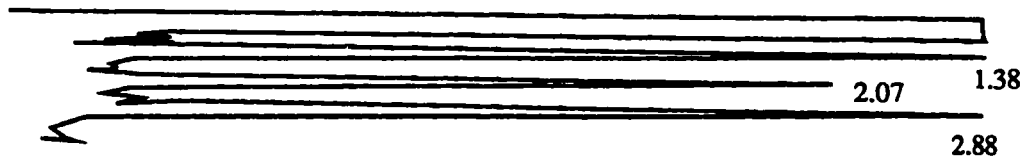

Figure 10: *Sample Chromatogram*: oxidation of DOPAC (retention time 1.38 min) in 20µl of a dialysis sample collected from the rat NAS..

The system was calibrated prior to each use with (Sigma, Canada) standards containing dopamine and DOPAC dissolved in aCSF. The response of the detector was linear in the range of dopamine (Figure 11) and DOPAC (Figure 12) concentrations analyzed. Based on the regression lines obtained the sensitivities and detection limits of the dopamine and DOPAC assays were calculated (appendix 1): dopamine; detection limit (2.2e-10 M) and sensitivity (8.4e+13 area/M) and DOPAC; detection limit (2.4e-8) and sensitivity (1.3e + 13 area/M).

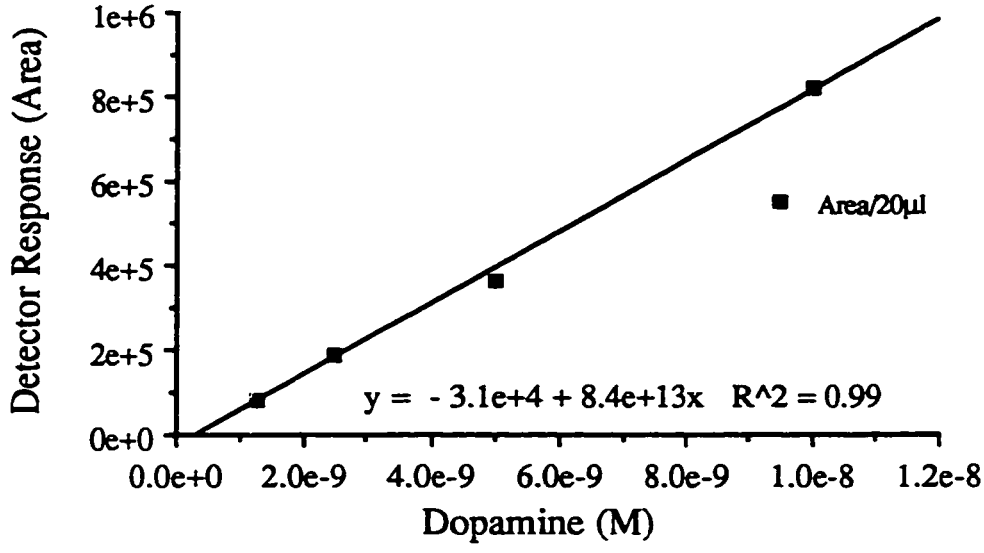

Figure 11: *Detector response Curve: reduction of dopamine quinone at -260nA.*

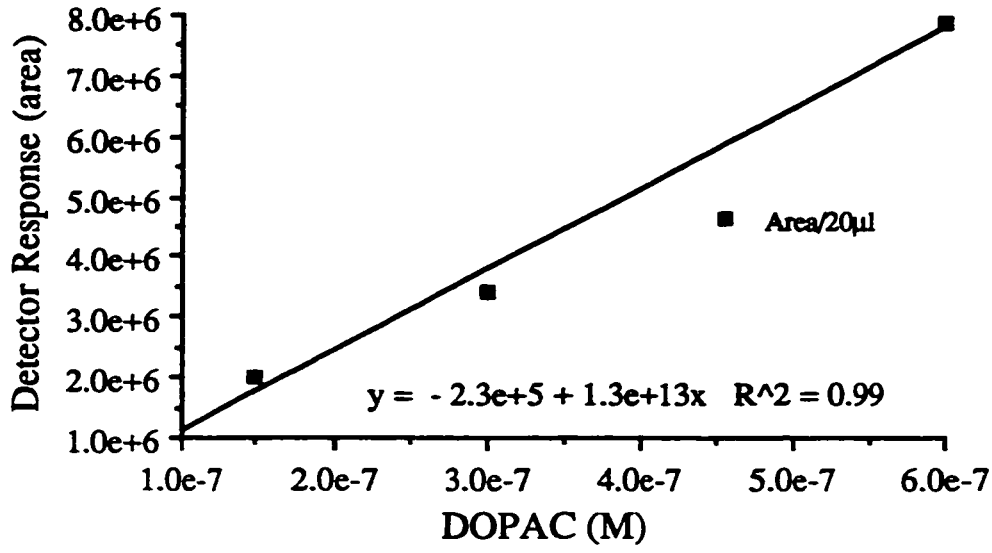

Figure 12: *Detector response curve: oxidation of DOPAC at +340 nA.*

The data were captured from the integrator (Spectra Physics 4270, Canada) to a 486 IBM-compatible computer. This was done using Spectra Physics Winner on Windows software, version 15.2.

2.2 Results

2.2.1 Reliability of glutamate

Eighteen aliquots of two dialysis samples, collected from probes implanted in the NAS, were derivatized and injected sequentially. There was no decay in sample glutamate content during the nine hours required to complete 18 injections of each sample (Figure 13). The average glutamate concentration of Sample 1 was 6.3 μM with a standard deviation of ± 0.4 μM; the average glutamate concentration of Sample 2 was 3.1 μM with a standard deviation of ± 0.3 μM.

2.2.2 Changes in sample composition following probe implantation

After implanting probes into the NAS glutamate and dopamine sample concentrations decreased with time indicating a similar decrease in extracellular dopamine and glutamate concentrations (Figure 14). This decrease continued for approximately 6 hours after implantation. Between 6 and 12 hours post implantation glutamate levels increased while dopamine levels stabilized. Levels of dopamine and glutamate were stable 12 to 16 hours post implantation.

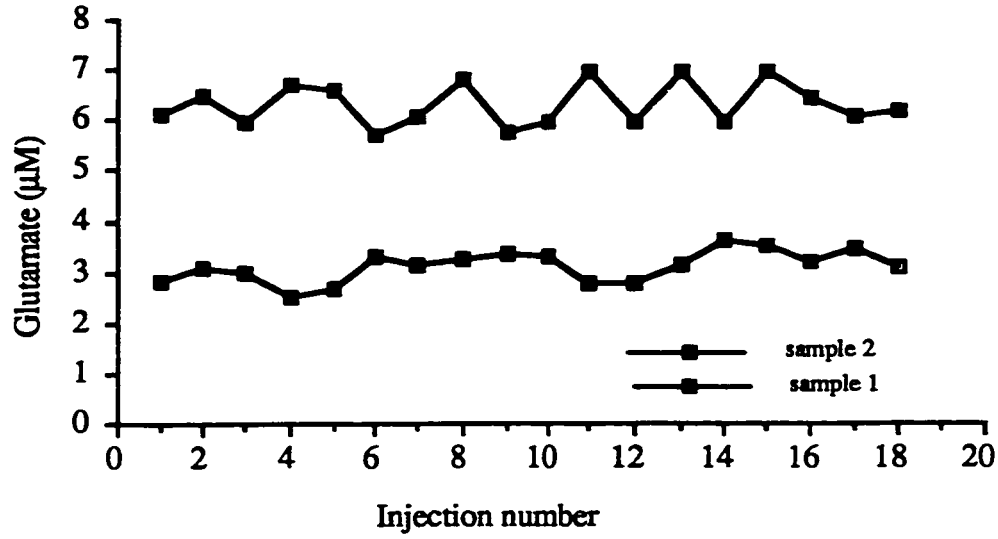

Figure 13: *Reproducibility of microdialysis sample glutamate analysis.* Eighteen aliquots of each dialysis sample (Sample 1 and Sample 2) were preloaded into vials and injected sequentially on to the column at 30 minute intervals.

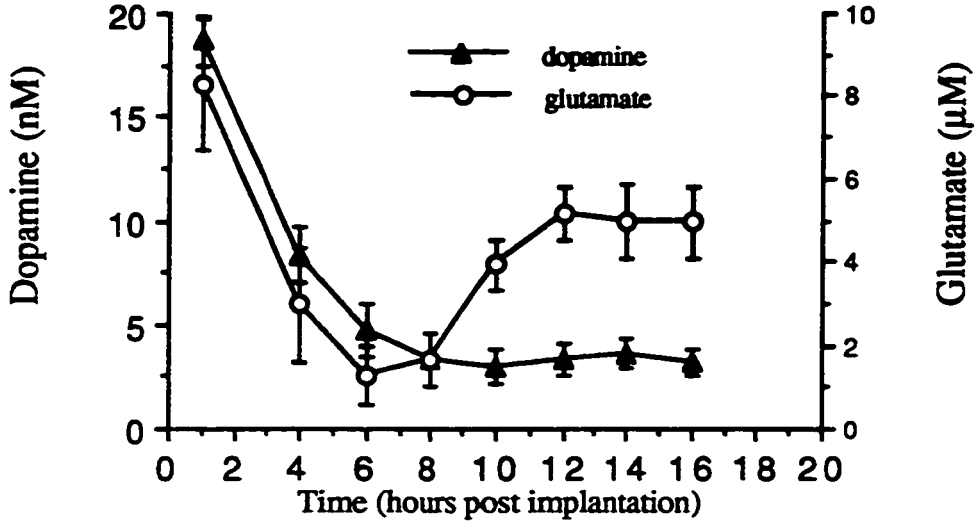

Figure 14: *Changes in sample dopamine and glutamate concentrations following probe implantation.* Sample concentrations of dopamine and glutamate during the first 16 hours following probe implantation (flow rate 0.5 μl/min, n=6). Error bars represent standard error of the mean (Appendix 2).

2.3 Discussion

2.3.1 Reliability of glutamate measures

The standard deviation of the glutamate assay used for this study was ± 0.4 μM. This value was used to calculate the sensitivity of the assay for detecting changes in sample glutamate concentration. Deviations from the basal sample glutamate concentration greater than ± 0.8 μM were considered significantly different from the variation between sequential analyses of identical samples. The standard deviation between analyses of identical samples was assessed frequently and used as an index of the working condition of the system. During sequential assays there was no trend of change in glutamate concentration, indicating that the reagents used for derivatizing glutamate and the dialysis samples were stable over the nine hour period required to assay 18 samples. An auto-injector run time of nine hours or less was used for all subsequent analyses.

2.3.2 Characterization of changes in NAS extracellular glutamate immediately following probe implantation.

Sample glutamate and dopamine concentrations were higher 2 hours after probe implantation than they were 6 to 8 hours later (Figure 14). This decrease in sample dopamine concentration has been well documented and is thought to be related to tissue damage that occurs during probe implantation. Specifically it has been suggested that dopamine diffuses out of nerve terminals damaged during probe implantation (Drew *et al.*, 1989; Shuaib *et al.*, 1990). The decreases in dopamine and glutamate concentrations that occurred during the first 8 to 9 hours following implantation have similar time courses, suggesting that they may occur by similar mechanisms. Glial cells and glutamatergic terminals of the NAS each contain high intracellular concentrations of glutamate. Like dopaminergic terminals, glia and glutamatergic terminals may incur physical damage during probe implantation, causing an increase in the diffusion of glutamate from these cells. Alternately these changes in glutamate and dopamine levels

may be related to the stabilization of gradients following the initial extraction of dopamine and glutamate from the tissue. This possibility could be tested by waiting 12 hours (post implantation) before pumping perfusate through the probe and monitoring changes in sample glutamate and dopamine concentrations that occur when perfusate flow is initiated.

While dopamine levels stabilized, a gradual increase in glutamate levels occurred 6 to 12 hours after implantation. This increase may be related to changes in glial cell activity that occur 6 to 12 hours following probe implantation (Shuaib *et al.*, 1990; Woodroofe *et al.*, 1991) . Glial cells swell and proliferate following implantation (section 2.0.3, pg. 14) and swelling of glial cells can inhibit or reverse the transport of glutamate across glial cell membranes (Hansson and Ronnback, 1995; Patterson *et al.*, 1995). This decrease in glutamate uptake by glia results in accumulation of glutamate released into the extracellular fluid. The increase in extracellular glutamate that occurs 6 to 12 hours following probe implantation may be associated with the influence of glial swelling on glutamate transport. This hypothesis could be investigated by monitoring changes in extracellular glutamate that occur following probe implantation in the presence of drugs that influence glial swelling or glutamate uptake.

Chapter 3

Analysis of NAS extracellular glutamate concentration

3.0 Introduction

The aim of the present experiments was to estimate the extracellular glutamate concentration in the NAS and to determine if disturbances of that concentration influence the extracellular dopamine concentration. Microdialysis sampling disturbs the extracellular concentrations of neurotransmitters by depleting them. Two methods (no-net-flux and extrapolation-to-zero-flow) have been proposed to obtain estimates of "undisturbed" extracellular neurotransmitter concentrations from microdialysis data. The method of no-net-flux involves estimating the undisturbed extracellular analyte concentration by finding the perfusate analyte concentration that is at equilibrium with the extracellular concentration. The extrapolation-to-zero-flow method involves extrapolating the equilibrium analyte concentration from the analyte concentrations of samples collected at a series of flow rates.

3.0.1 No-net-flux estimation

The undisturbed extracellular concentration can be estimated from the relationship between the inlet analyte concentration and the net diffusion of analyte across the membrane (Lonnroth, P. et al., 1987). The diffusion of analyte across the membrane can be influenced by changing the inlet analyte concentration (Ci). Changes in the inlet analyte concentration alter the initial concentration difference across the membrane leading to a change in the rate and perhaps the direction of analyte diffusion. If the inlet analyte concentration is greater than the extracellular analyte concentration (Cec) there will be a net diffusion of analyte into the extracellular fluid (delivery); in this case the difference between Ci and final sample concentration (Cs) will be greater than zero (Ci-

Cs>0). If the inlet analyte concentration is less than the extracellular analyte concentration there will be a net diffusion of analyte into the perfusate (extraction); in this case the difference between Ci and Cs will be less than zero (Ci-Cs<0). If the inlet concentration is equal to the extracellular concentration there will be no concentration difference across the membrane and no net diffusion of analyte across the membrane (no-net-flux). Under this condition, the concentration of analyte in the perfusate will be at equilibrium with the local extracellular fluid and there will be no change in the analyte concentration of the perfusate as it flows through the probe (Ci-Cs=0). The equilibrium concentration estimates the undisturbed extracellular analyte concentration; thus the undisturbed extracellular analyte concentration can be obtained from the regression line that expresses the relationship between net analyte flux across the membrane and inlet analyte concentration (Figure 15).

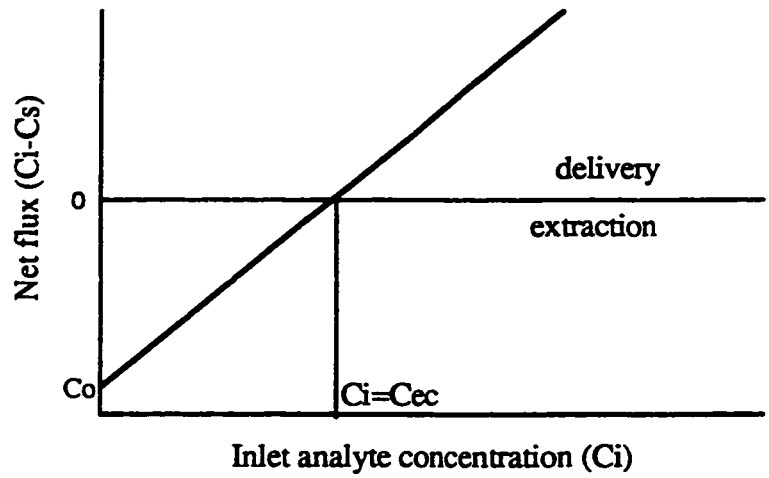

Figure 15: *No-net-flux estimation of an undisturbed extracellular analyte concentration.* The undisturbed extracellular analyte concentration is estimated by value of Ci when the net analyte diffusion equals 0 which is estimated based on the line (Ci-Cs) = m(Ci)+Co obtained by linear regression analysis. Co is the sample analyte concentration when Ci equals zero.

3.0.2 Extrapolation to zero flow estimation

Equilibration between the perfusate and the extracellular fluid can also be increased by decreasing the rate of perfusate flow through the probe (Section 1.1.4) (Jacobson *et al.*, 1985; Lindefors *et al.*, 1989). A change in flow rate alters the degree of equilibration between the perfusate and extracellular fluid by altering the time allowed for equilibration between the perfusate and the extracellular fluid. At slower flow rates more time is allowed for equilibration between the perfusate and the extracellular fluid. As flow rate approaches zero the time allowed for equilibration between the perfusate and the extracellular fluid approaches infinity. At zero flow, the sample concentrations of extracellular compounds that diffuse into the perfusate eventually approach the extracellular concentrations of the same compounds. However, no sample is collected at zero flow. As a result, estimating the undisturbed extracellular concentration from the relationship between flow rate and sample concentration requires extrapolation from yields of successive samples obtained at flow rates that represent a compromise between increasing equilibrium and collecting a measurable sample .

3.1 Methods

See section 2.1 pg. 15 for information regarding: animal care, surgery, microdialysis procedure and biochemical assays.

3.1.1 In vitro estimation of bath glutamate concentration

Before implantation, each probe was tested *in vitro* using either the no-net-flux method or the extrapolation-to-zero-flow method. This calibration was done while probes were immersed in a stirred 5.0 ± 0.4 μM glutamate solution at room temperature. The glutamate solutions were made daily using aCSF as the solvent; the pH of each solution was adjusted to 7.2-7.4 with sodium hydroxide (Sigma, Canada) following the addition of D-glutamate (Sigma, Canada).

The no-net-flux estimate of the glutamate concentration of the 5.0 ± 0.4 μM glutamate solution was obtained by perfusing a range glutamate concentrations (0, 2.4 ± 0.5 μM, 4.9 ± 0.4 μM, 8.0 ± 0.3 μM, and 10.0 ± 0.4 μM) and calculating the net diffusion of glutamate between the perfusate and the solution (n=6). Following equilibration at each C_i three ten-minute samples were collected and frozen with dry ice. The net dialysis of glutamate was calculated as the difference between the initial and sample glutamate concentrations (C_i-C_s). The relationship between these variables, net dialysis of glutamate and C_i, was analyzed by linear regression. The influence of changes in perfusate flow rate on this estimate was investigated by estimating the glutamate concentration of the solution at two flow rates 0.5 μl/m and 1.0 μl/m.

Samples were also collected from probes bathed in a 5.0 ± 0.4 μM glutamate solution at a series of perfusate flow rates. The perfusate (0 μM glutamate) was pumped (Harvard syringe pump) through the probes at flow rates of 0.25 μl/m, 0.5 μl/m, 1.0 μl/m, 1.5 μl/m and 2.0 μl/m. Following equilibration at each flow rate three samples were collected at 10 minute intervals and frozen immediately with dry ice.

3.1.2 Determining the undisturbed NAS glutamate concentration

Probes implanted in the NAS of conscious rats (n=6) were perfused with a range of inlet glutamate concentrations (0 μM, 1.0 ± 0.4 μM, 2.1 ± 0.4 μM, 4.0 ± 0.5 μM, 4.9 ± 0.4 μM, 6.1 ± 0.5 μM, 8.0 ± 0.3 μM). The C_i was changed at the swivel; each change entailed momentarily stopping the flow of perfusate through the probe. Twenty minutes were allowed for equilibration of the system following each change of perfusate concentration. The net diffusion of glutamate across the membrane was calculated as Cs-Ci and the undisturbed extracellular concentration was estimated from the relationship between net glutamate dialysis and the inlet glutamate concentration. This relationship was represented by a regression line with the equation, (Ci-Cs)=m(Ci)-Co. To determine the influence of the rate of dialysis on the no-net-flux estimate, the no-net-flux concentration was estimated at two flow rates 1.0 μl/m and 0.5 μl/m.

The relationship between the dialysis of glutamate and the perfusate flow rate was also investigated. Samples were collected at a range of perfusate flow rates (0.25 μl/m, 0.5 μl/m, 1.0 μl/m, 1.5 μl/m, and 2.0 μl/m) during the perfusion of aCSF (0 μM glutamate) through probes implanted in the NAS. A 20 minute equilibration time was allowed following each change in flow rate. Samples were collected at each flow rate and frozen immediately on dry ice. The sample concentration at zero flow was not estimated because insufficient data were collected at slower flow rates.

3.2 Results

3.2.1 In vitro no-net-flux glutamate

The concentration of the probe bath (5.0 ± 0.4 μM glutamate solution) was estimated at two flow rates (Figure 16). At each flow rate there was a linear relationship between the net diffusion of glutamate and the inlet glutamate concentration regardless of the direction of analyte diffusion ($R^{\wedge 2} = 0.99$; 0.5 μl/m and $R^{\wedge 2} = 0.98$; 1.0 μl/m). The undisturbed bath concentration of glutamate was estimated at two perfusate flow rates; at a flow rate of 0.5 μl/m the estimate was 5.1 μM ($\sigma_X = 0.5$) and at a flow rate of 1.0 μl/m the estimate was 4.7 μM ($\sigma_X = 0.9$). These estimates do not differ by a factor greater than the uncertainty (σ_X) of each estimate (Appendix 3). The average of these estimates gives a glutamate concentration of 4.9 μM ($\sigma_X = 0.7$). The slopes of the regression lines (Δ net dialysis/ΔC_i) varied inversely with flow rate. The change in net dialysis relative to a change in the analyte gradient was greater at the slower flow rate; the slope was 0.57 ($\sigma_m = 0.02$) at a flow rate of 0.5 μl/m and 0.36 ($\sigma_m = 0.02$) at a flow rate of 1.0 μl/m (Figure 16).

3.2.2 In vitro flow rate studies

The sample concentration of glutamate and equilibration of the glutamate concentration difference across the membrane varied inversely with perfusate flow rate (Figure 17). At the lowest flow rate tested the sample was 88% equilibrated with the bath fluid outside the probe; at a flow rate of 0.25 μl/m the sample glutamate concentration was 4.4 ± 0.3 μM. However, an estimate of the extracellular glutamate concentration based on the sample glutamate concentration at zero flow was not obtained. The data could not be analyzed by non-linear regression and estimation of the concentration at zero flow was not possible.

3.2.3 In vivo no-net-flux NAS glutamate

At both perfusate flow rates tested (0.5 µl/m and 1.0 µl/m) there was a linear relationship between the inlet perfusate concentration and the net dialysis of glutamate into or out of the perfusate ($R^{\wedge 2} = 0.96$; 0.5 µl/m and $R^{\wedge 2} = 0.97$; 1.0 µl/m) (Figure 18). The undisturbed glutamate concentration of the NAS extracellular fluid was estimated at 3.8 µM ($\sigma_x = 0.8$) at a flow rate of 0.5 µl/m, and 4.2 µM ($\sigma_x = 0.9$) at a flow rate of 1.0 µl/m. These concentrations do not differ by a factor greater than the uncertainty (σ_x) of each estimate (Appendix 3). The average of these two estimates gives an extracellular glutamate concentration of 4.0 µM ($\sigma_x = 0.8$). The slopes of the regression lines (Δ net dialysis/ΔC_i) varied inversely with flow rate. The change in net dialysis relative to a change in the analyte gradient was greater at the slower flow rate; the slope was 1.18 ($\sigma_m = 0.10$) at a flow rate of 0.5 µl/m and 0.67 ($\sigma_m = 0.07$) at a flow rate of 1.0 µl/m (Figure 18).

3.2.4 Effect of glutamate dialysis on sample dopamine and DOPAC content

The no-net-flux estimations required perfusing glutamate concentrations higher than and lower than the extracellular glutamate concentration. As a result glutamate was delivered to the extracellular fluid or extracted from extracellular fluid during collection of the no-net-flux data. The depletion or delivery of NAS glutamate within the range of rates tested did not cause a significant change in the dopamine concentration of dialysis samples collected during the no-net-flux experiment (Figure 19). Furthermore this depletion or delivery of NAS glutamate was not associated with a significant change in the sample concentration of DOPAC a metabolite formed by metabolism of dopamine within dopaminergic neurons (Figure 20).

3.2.5 In vivo flow rate studies

Samples were collected *in vivo* at four flow rates (2.0 µl/min, 1.0 µl/m, 0.5 µl/m and 0.25 µl/min), and sample glutamate and dopamine concentrations varied inversely with perfusate flow rate (Figure 21, Figure 22, respectively). At the slowest flow rate tested (0.25µl/min) the sample glutamate concentration was 5.1 ± 0.6 µM, indicating that the undisturbed extracellular glutamate concentration in the NAS is greater than or equal to 5.1 ± 0.6µM. Similarly, at a flow rate of 0.25 µl/min the sample dopamine concentration was 4.6 ± 0.3 nM, suggesting that the undisturbed extracellular dopamine concentration is greater than 4.6 ± 0.3 nM.

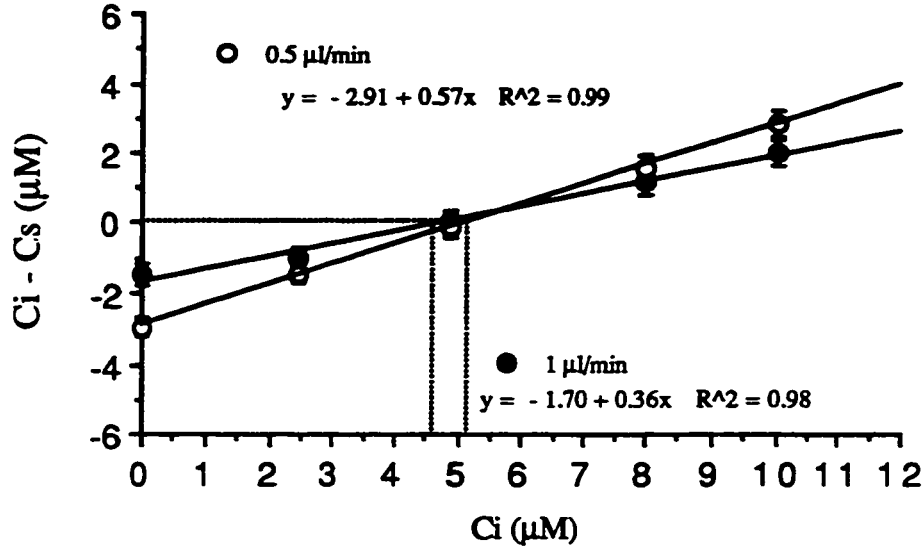

Figure 16: *Determination of undisturbed glutamate concentration in vitro.* The relationship between the net dialysis of glutamate (Ci-Cs) and the inlet glutamate concentration (Ci) was determined at two flow rates: 0.5 µl/min and 1 µl/min (n=6). Error bars represent standard error of the mean (Appendix 2).

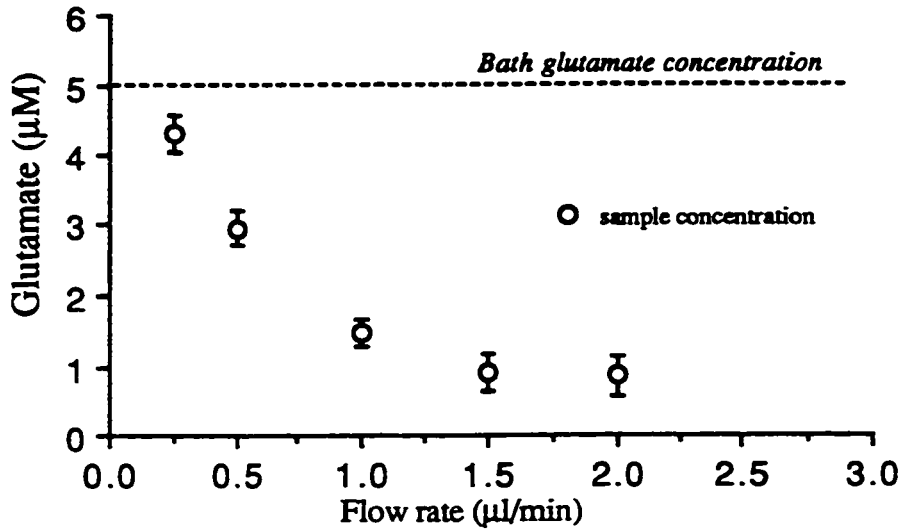

Figure 17: *In vitro relationship between flow rate and sample glutamate concentration.* The initial perfusate glutamate concentration was 0 µM throughout the experiment. Horizontal line represents glutamate concentration of probe bath. Error bars represent standard error of the mean (Appendix 2).

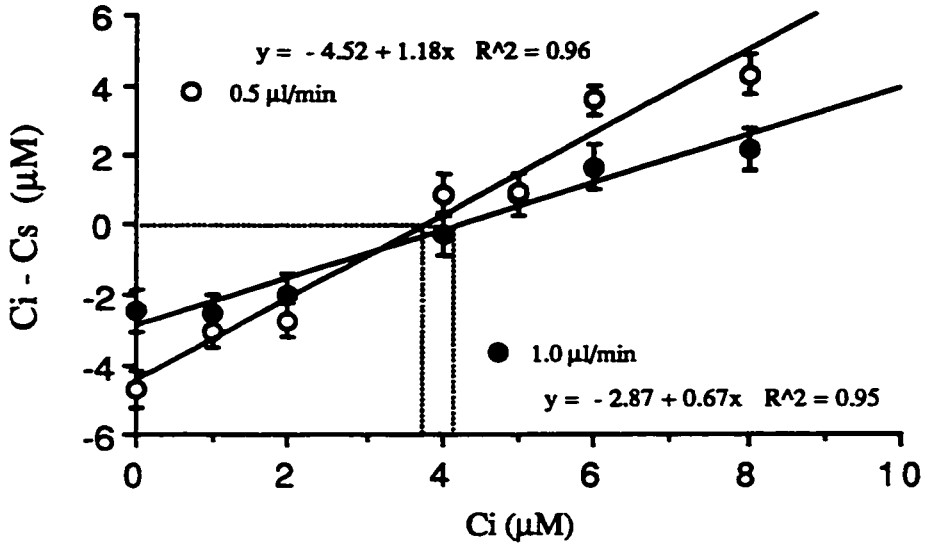

Figure 18: *Estimation of undisturbed extracellular glutamate concentration of NAS.* The net dialysis of glutamate (Ci-Cs) across the membrane of probes implanted into the NAS was determined at two flow rates: 1.0 µl/min and 0.5 µl/min (n=6). Error bars represent standard error of the mean (Appendix 2).

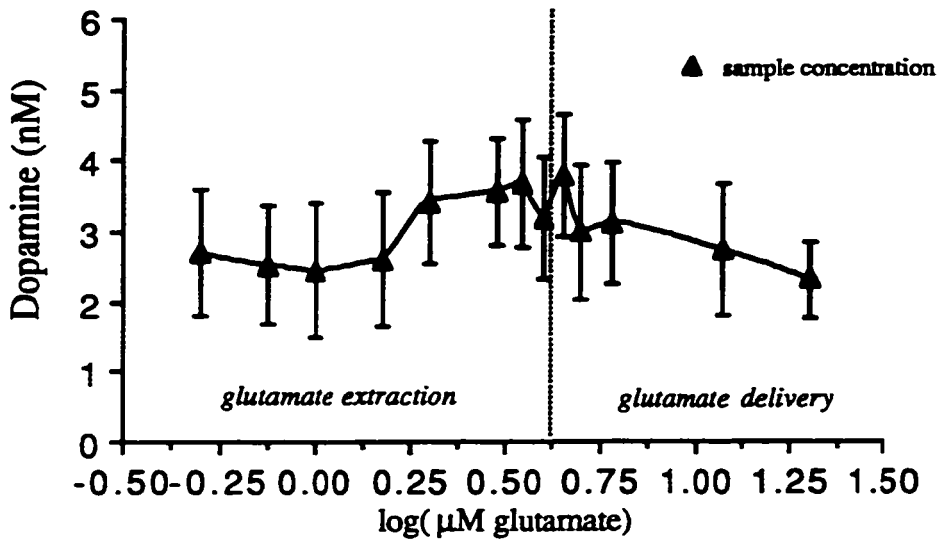

Figure 19: *Effect of glutamate perfusion on sample dopamine concentration* (n=5). At perfusate glutamate concentrations less than the estimated extracellular glutamate concentration (4 μM, 0.6 log units), glutamate is extracted from the extracellular fluid of the NAS. At perfusate concentrations greater than 4 μM glutamate is delivered to the extracellular fluid. Error bars represent standard error of the mean (Appendix 2).

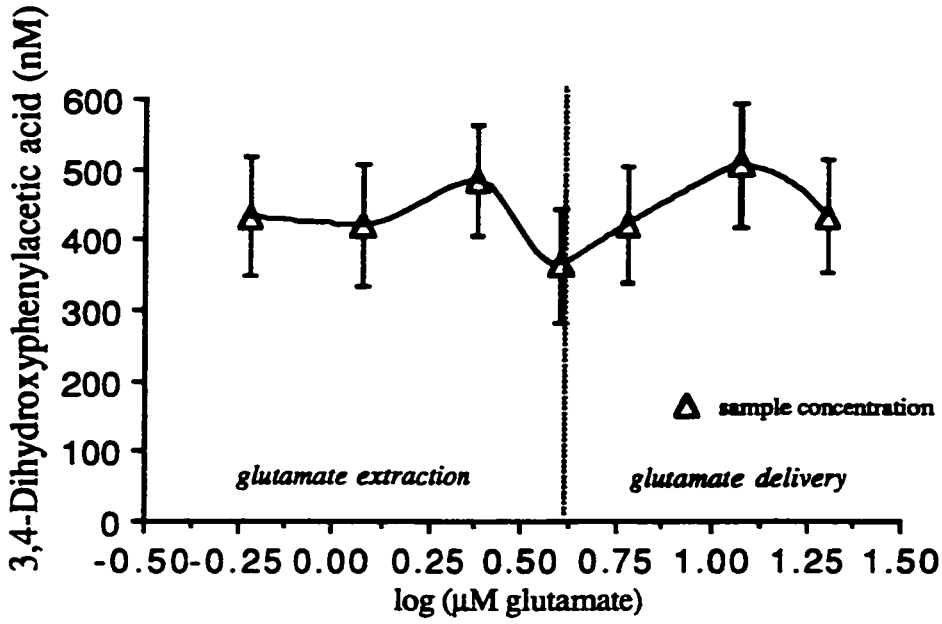

Figure 20: *Effect of glutamate perfusion on sample DOPAC concentration* (n=5). At perfusate glutamate concentrations less than the estimated extracellular glutamate concentration (4 μM, 0.6 log units), glutamate is extracted from the extracellular fluid of the NAS. At perfusate concentrations greater than 4 μM glutamate is delivered to the extracellular fluid. Error bars represent standard error of the mean (Appendix 2).

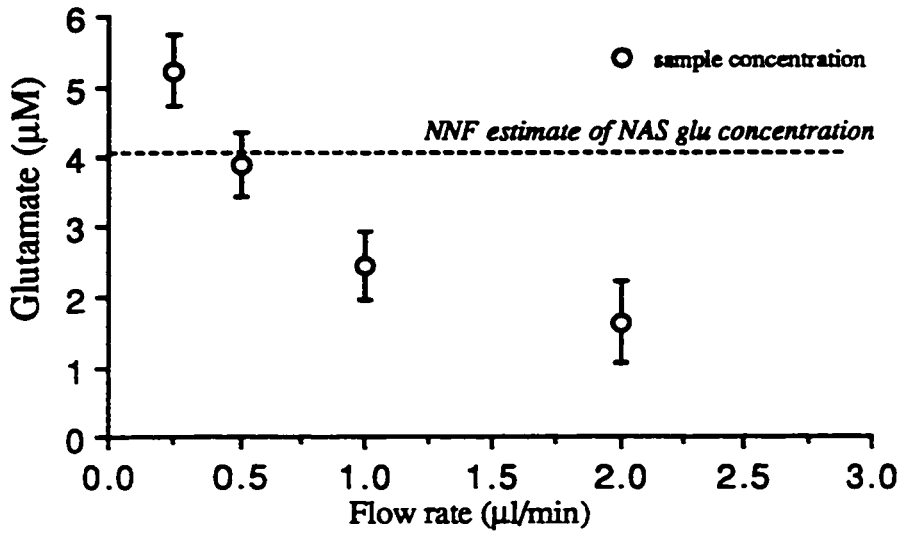

Figure 21: *In vivo-relationship between perfusion flow rate and sample glutamate concentration.* The initial perfusate glutamate (glu) concentration was zero throughout the no-net-flux experiment. Dashed horizontal line represents no-net-flux (NNF) estimate of glutamate (glu) concentration (Figure 16, pg 38). Error bars represent standard error of the mean (Appendix 2).

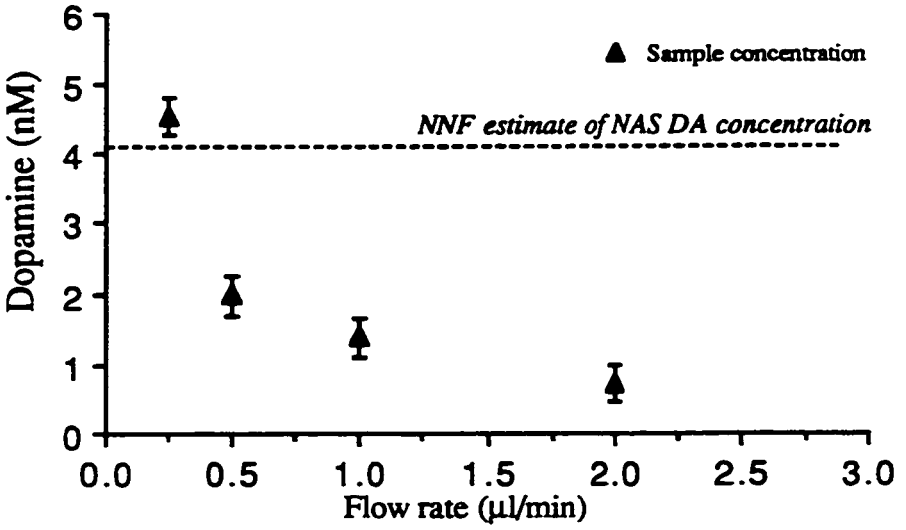

Figure 22: *In vivo-relationship between perfusion flow rate and sample dopamine concentration.* The initial perfusate dopamine (DA) concentration was zero throughout the experiment. Dashed horizontal line represents no-net-flux (NNF) estimate of dopamine (DA) concentration (Parsons and Justice, 1992). Error bars represent standard error of the mean (Appendix 2).

3.3 Discussion

3.3.1 Estimation of glutamate concentration

The no-net-flux study gave an estimate of 4.0 ± 0.8 μM for the undisturbed extracellular concentration of glutamate. The extrapolation-to-zero-flow method did not yield convincing evidence of an upper limit, but suggested a somewhat higher value; this method suggested that a concentration of at least 5.1 ± 0.6 μM was present in the NAS of animals tested. These estimates are reasonably consistent with one another and with other microdialysis-based estimates of the brain extracellular glutamate concentration.

Miele et al., (1996) estimated the extracellular glutamate concentration of the caudate nucleus at 3.0 μM. This no-net-flux estimate is slightly lower but close to the estimates of NAS extracellular concentration obtained in the present study. This similarity is not unexpected considering the anatomical and physiological similarity of the caudate nucleus and the NAS, the dorsal and ventral (respectively) divisions of the striatum. Two other publications also contain microdialysis-based estimates of the extracellular glutamate concentrations of specific brain regions: in the rabbit hippocampus an estimate of 2.9 μM was obtained (Lerma *et al.*, 1986) using a recirculation method, and in the rabbit olfactory bulb an estimate of 4.3 μM was obtained using the extrapolation-to-zero-flow method (Jacobson *et al.*, 1985). The similarity of these estimates suggests that basal extracellular glutamate concentration may be controlled by similar physiological mechanisms in these three brain regions.

3.3.2 Glutamate dialysis is more efficient in vivo than in vitro

It is interesting that glutamate diffused across the dialysis membrane more efficiently *in vivo* than *in vitro* (compare Figure. 16, pg. 39 and Figure 18, pg. 41). The fact that the NAS was more able to accept and donate glutamate than was the stirred glutamate solution in a beaker suggests that some characteristics of the physiology of the tissue were more efficient in this respect than was the passive diffusion to or from the

stirred solution. It has been reported that the diffusion of the neurotransmitter dopamine into microdialysis probes is more efficient *in vivo* than *in vitro* and that the diffusion of the dopamine metabolite DOPAC is the same *in vitro* and *in vivo* (Parsons and Justice, 1992). Furthermore, the active uptake of dopamine and not DOPAC contributes to these differences in diffusion efficiency (Parsons, and Justice, 1994). These findings indicate that active exchange of glutamate across cell membranes delivers or scavenges glutamate from the extracellular fluid at the probe surface more efficiently than does passive diffusion in the stirred beaker. This active exchange includes, exocytotic release of neurotransmitter from nerve terminals, reuptake of neurotransmitter into neurons, and uptake of neurotransmitter into glia. In this context the present finding that glutamate dialysis is more efficient *in vivo* than *in vitro* indicates that the NAS extracellular glutamate pool sampled was actively exchanged between the intracellular and extracellular compartments. This is consistent with the facts that glutamate is released by exocytosis from glutamatergic terminals in the NAS and removed from the extracellular fluid by active transport into neurons and glia.

3.3.3 No-net-flux estimate was not influenced by an increase in nonspecific extraction.

It has been suggested that the extraction of dopamine, glutamate, or other small molecules during microdialysis should influence the activity of cells near the probe, altering local neurotransmitter release and concentrations (Blaha, 1991; Sam and Justice, 1996). At the no-net-flux point there is no net extraction or net delivery of glutamate. However, other extracellular constituents that are not contained in the perfusate are extracted. This extraction of "other" extracellular constituents can be increased by increasing the flow rate of perfusate through the probe. At higher flow rates the dialysate passes the active portion of the membrane more quickly, allowing less time for equilibration. Because a greater volume is perfused in a given time, the concentration of the analyte in the dialysate decreases. However, at higher flow rates, reduced equilibration means that the concentration gradient across the membrane is maintained

more effectively leading to a greater absolute transfer of analyte to or from the dialysate. For example, increasing the flow rate from 0.5 µl/m to 1.0 µl/m caused a 30% increase in the extraction of NAS dopamine and glutamate However, increasing the flow rate from 0.5 µl/m to 1.0 µl/m did not significantly alter the no-net-flux estimate of NAS extracellular glutamate concentration, indicating that this increase in "nonspecific" extraction of neurotransmitters did not significantly influence the activity of glutamate releasing cells in the tissue depleted by dialysis.

3.3.4 Extraction or depletion of NAS glutamate during no-net-flux estimation did not influence extracellular concentration of dopamine

The sample dopamine concentration was monitored during the perfusion of solutions with glutamate concentrations higher and lower than the undisturbed extracellular glutamate concentration of the NAS. Changes in the delivery or extraction of extracellular glutamate associated with these perfusate glutamate concentrations did not lead to significant changes in the sample dopamine concentration. This finding suggests that the activity of NAS dopamine releasing cells was not affected by the increases or decreases in extracellular glutamate concentration caused by perfusing glutamate concentrations greater than or less than the extracellular glutamate concentration. Furthermore, sample DOPAC levels were not affected by changes in glutamate extraction or delivery, indicating that the metabolism of dopamine to DOPAC by dopaminergic neurons was not affected by this treatment.

3.3.5 The range 3.5 3.2-5.6 µM is consistent with the responsiveness of glial glutamate transporters to glutamate

The estimates obtained in this study indicate that the extracellular glutamate concentration in the rat NAS is approximately 3.2-5.6 µM. Glutamate is removed from the extracellular fluid by active transport into glia and neurons. The balance between neuronal glutamate release and the uptake of glutamate by neurons and glia appears to determine the basal extracellular glutamate concentration (Herrera-Marshchitz *et al.*, 1996). Neuronal glutamate transporters respond to glutamate at concentrations in the low

mM range while glial glutamate transporters respond to glutamate at concentrations in the low μM range (Klockner *et al.*, 1993). Because glial glutamate transporters are activated by lower glutamate concentrations than are neuronal transporters, glial transport is thought to have the prominent role in maintaining the brain extracellular glutamate levels and would be expected to maintain extracellular glutamate levels in the low μM range (Szatkowski *et al.*, 1990; Bouvier *et al.*, 1992). The present findings support this suggestion; the estimate obtained is within the concentration range that could be maintained by glial glutamate transport, much lower than the range that could be maintained by neuronal glutamate transport. Various other findings also indicate that glial transport is important for the maintenance of glutamate levels in the brain. For example, glial glutamate transporters are highly expressed in brain regions that have extensive glutamatergic input (Hansson and Ronnback 1995) and approximately 85% of glutamate released by neurons is taken up by glial cells (McKenna *et al.*, 1996). Furthermore, glial metabolism of glutamate is necessary for maintenance of normal levels of glutamate in glutamatergic terminals (Laake *et al.*, 1995)

3.3.6 Estimate obtained in this study is reasonable in context of what is known about NAS glutamatergic neurotransmission

The present estimate of the NAS extracellular concentration is reasonable in the context of the responsiveness of NAS glutamate receptors to extracellular glutamate. This suggests that the glutamate signal monitored using microdialysis is biologically relevant and that the microdialysis procedure itself does not cause a dramatic change in the extracellular glutamate concentration in the vicinity of the probe.

Glutamate neurotransmission in the NAS is mediated by at least three types of glutamate receptors: N-methyl-D-aspartate (NMDA) receptors, a-amino-3-hydroxy-5-methyl-isoxazole-4-propionate (AMPA) receptors, and metabotropic glutamate receptors. The NAS contains dense populations of NMDA, AMPA and metabotropic receptors (Albin *et al.*, 1992). and numerous variants of each of these receptor types are located in

the plasma membranes of NAS neurons and glia (Albin *et al.*, 1992; Hollmann and Heinemann, 1994).

The estimated extracellular glutamate concentration is high enough to activate most NMDA receptor subtypes, suggesting possible activation of NAS NMDA receptors under basal conditions. NMDA receptors are most responsive to glutamate at concentrations between 0.72 μM and 5.6 μM (Moriyoshi *et al.*, 1991; Durand *et al.*, 1992; Sekiguchi *et al.*, 1992). But, basal levels of NAS glutamate may not activate NMDA receptors; NMDA receptor activation requires not only the binding of glutamate but also the binding of other ligands as well as concurrent membrane depolarization. AMPA receptors are activated by glutamate at concentrations higher than the predicted NAS glutamate concentration; AMPA receptors are most responsive to concentrations of glutamate between 9.2 μM and 32.3 μM (Sakimura *et al.*, 1990; Moriyoshi *et al.*, 1991; Stein *et al.*, 1992). However, it is important to consider that microdialysis reflects the average analyte concentration both over the time of collection and over the area reached by the dialysis-imposed concentration gradients. As a consequence this method is relatively insensitive to brief or localized glutamate release in response to specific signals or events; thus transient or localized increases in extracellular glutamate concentration may not lead to changes in sample glutamate concentration. AMPA receptors may be located within the synapse where these transient increases in glutamate concentration occur.

Both NMDA and AMPA receptors respond best to transient increases in glutamate concentration; desensitization of NMDA and AMPA responses occurs if the glutamate concentration is maintained above a critical level for an extended period of time. AMPA receptors are more sensitive in this respect than NMDA receptors. The responsiveness of AMPA receptors to glutamate is decreased by 50% following prolonged exposure to glutamate concentrations between 3 μM and 9.6 μM (Jonas,

1993). The present findings suggest that AMPA receptors may be partially desensitized by basal levels of extracellular glutamate.

Metabotropic glutamate receptor subtypes, mGluR3, mGluR2, mGluR1, mGluR5 reside on NAS neurons and glia but only mGluR3 receptors are sensitive to concentrations close to the estimated basal glutamate concentration (4 μM) (Pin. and Duvoisin, 1995). Metabotropic glutamate receptors mGluR3 and mGluR2 are thought to mediate presynaptic depression of cortical glutamatergic inputs to the NAS (Lovinger and McCool, 1995) . MGluR2 and mGluR3 receptors are most responsive to 4 μM glutamate and 12 μM glutamate respectively. Basal NAS glutamate levels (4μM) may activate mGluR3 receptors on glutamatergic terminals, leading to the tonic inhibition of NAS glutamate release.

4.0 Summary and Conclusions

The objectives of this study were to characterize and to estimate the "undisturbed" extracellular concentration of glutamate and to investigate the effects of dialysis on extracellular levels of dopamine, DOPAC and glutamate. For this purpose an assay using HPLC and electrochemical detection was established and the stability of the glutamate measures was studied as a function of time after probe implantation.

The "undisturbed" extracellular glutamate concentration was estimated at 4.0 ± 0.8 μM. An estimate of 5.1 ± 0.6 μM was obtained by studying the relationship between flow rate and glutamate extraction. From these experiments a concentration range of 3.2-5.6 μM is identified as the "undisturbed" extracellular level of glutamate in the rat NAS. This concentration range is consistent with other estimates of brain extracellular glutamate concentration. In addition this estimate is reasonable considering the activity of NAS glutamate receptors and uptake systems, attesting to the biological relevance of glutamate in the NAS during microdialysis.

NAS extracellular glutamate levels were not influenced increased non-specific extraction of extracellular compounds (other than glutamate) caused by an increase in dialysis flow rate. The "undisturbed" glutamate concentration was the same at both flow rates tested (0.5 μl/m and 1.0μl/m). Similarly, sample levels of dopamine or DOPAC were stable throughout the no-net-flux estimation; the extraction or delivery of glutamate that occurred during the perfusion of a range of glutamate concentrations did not influence extracellular levels of dopamine or DOPAC.

5.0 Appendices

5.1 Appendix 1: calculation of detection limit.

slope of calibration curve (m); uncertainty of the y intercept (σ_b); square root of (sqrt)

sensitivity = m

detection limit = $2 \times (\sigma_b) / m$

standard deviation of y (s_y); measured y values (y_i); predicted y values (y_p)

$$s_y = \Sigma (y_i - y_p)^2 / (n-2)$$

$$\sigma_b = ((s_y)^2 \times \Sigma (x_i^2)) / D$$

$$D = n\Sigma (x_i)^2 - (\Sigma x_i)^2$$

5.2 Appendix 2: standard error of the mean.

standard error of the mean (σ_s)

$$\sigma_s = s_y / \text{sqrt}(n)$$

$$s_y = \Sigma (y_i - y_p)^2 / (n-2)$$

5.3 Appendix 3: calculation of uncertainty of no-net-flux estimate (x at y = 0)

standard deviation of y (s_y); measured y values (y_i); predicted y values (y_p)

$$s_y = \Sigma (y_i - y_p)^2 / (n-2)$$

uncertainty of the slope (σ_m)

$$\sigma_m = n(s_y^2)/D$$

$$D = n\Sigma (x_i)^2 - (\Sigma x_i)^2$$

uncertainty of y intercept (σ_b)

$$\sigma_b = ((s_y)^2 \times \Sigma (x_i^2)) / D$$

$$D = n\Sigma (x_i)^2 - (\Sigma x_i)^2$$

uncertainty of x at y = 0 (σ_x)

$$(\sigma_x/x)^2 = \text{sqrt}((s_y^2) + (\sigma_b^2)/y\text{-}b) + (\sigma_m^2/m^2)$$

6.0 Bibliography

Albin, R.L., Markowiec, R.L., Hollingsworth, Z.R., Dure, L.S., Penny, J.B. and Young, A.B. (1992). Excitatory amino acid binding sites in the basal ganglia of the rat: a quantitative autoradiographic study. *Neuroscience*, **46(1)**, 35-56.

Allison, L.A., Mayer, G.S. and Shoup, R.E. (1984). O-phthaladehyde derivatives of amines for high speed liquid chromatography/electrochemistry. *Analytical Chemistry*, **56(7)**, 1089-1096.

Benveniste, H. (1989). Brain Microdialysis. *Journal of Neurochemistry*, **52(6)**, 1667-1677.

Bianchi, L., Sharp, T., Bolam, J.P. and Corte, L.D. (1994). The effect of kainic acid on the release of GABA in rat neostriatum and substantia nigra. *Neuroreport*, **5**, 1233-1236.

Blaha, C.D. (1991). Monitoring Molecules. Fifth International Conference on *In vivo* Methods "Monitoring Molecules in Neuroscience", Noordwijkerhout, The Netherlands,

Bouvier, M., Szatkowski, A.A., Amato, A. and Attwell, D. (1992). The glial cell glutamate uptake carrier counter transports pH-changing anions. *Nature*, **360**, 471-474.

Burns, L.H., Everitt, B.J., Kelley, A.E. and Robbins, T.W. (1994). Glutamate-dopamine interactions in the ventral striatum: role in locomotor activity and responding with conditioned reinforcement. *Psychopharmacology*, **115**, 516-528.

Camp, D.M. and Robinson, T.E. (1992). On the use of multiple probe insertions at the same site for repeated intracerebral microdialysis experiments in the nigrostriatal dopamine system of rats. *Journal of Neurochemistry*, **58(5)**, 1706-15.

Campbell, K., Kalen, P., Lundberg, C., Wictorin, K., Rosengren, E. and Bjorklund, A. (1993). Extracellular g-aminobutyric acid levels in the rat caudate-putamen: monitoring the neuronal and glial contribution by intracerebral microdialysis. *Brain Research*, **614(1-2)**, 241-250.

Donzanti, B.A. and Yamamoto, B.K. (1988). An improved and rapid HPLC-EC method for the isocratic separation of amino acid neurotransmitters from brain tissue and microdialysis perfusates. *Life Science*, **(43)**, 913-922.

Drew, K.L., O'Connor, W.T., Kehr, J. and Ungerstedt, U. (1989). Characterization of g-aminobutyric acid and dopamine overflow following acute implantation of a microdialysis probe. *Life Science*, **45(14)**, 1307-1317.

Durand, G.M., Gregor, P., Zheng, X., Bennett, M.V., Uhl, G.R. and Zukin, R.S. (1992). Cloning of an apparent splice variant of the NMDAR1 with altered sensitivity of polyamines and activators of protein kinase C. *Proceedings of the National Academy of Science USA*, **(90)**, 9359-9363.

ESA, Inc. (1988). The Model 5100A Coulochem Detector Instruction Manual. Bedford, Massachusetts.

Fallon, J.H. (1988). Topographic organization of ascending dopaminergic projections. *Annuals of the New York Academy of Science,* **537**, 1-9.

Fallon, J.H. and Moore, R.Y. (1978). Catecholamine innervation of the basal forebrain. IV. Topography of the dopamine projection to the basal forebrain and neostriatum. *Journal of Comparative Neurology,* **180**, 545-580.

Fonnum, F. (1993). Regulation of the synthesis of the transmitter glutamate pool. *Progress in Biophysics and Molecular Biology,* **60**, 47-57.

Fuller, T.A., Russchen, F.T. and Price, J.L. (1987). Sources of presumptive glutamatergic/aspartergic afferents to the rat ventral striatopallidal region. *Journal of Comparative Neurology,* **258**, 317-338.

Fumero, B., Guadalupe, T., Valladares, F., Mora, F., O'Neill, R.D., Masu, M. and Gonzalez-Mora, J.L. (1994). Fixed versus removable microdialysis probes for *in vivo* neurochemical analysis: implications for behavioral studies. *Journal of Neurochemistry,* **63(4)**, 1407-1415.

Hamberger, A., Berthold, C.H., Karlsson, B., Lehmann, A. and Nystrom, B. (1983). Extracellular GABA, glutamate, and glutamine *in vivo* perfusion dialysis of the rabbit hippocampus. In: *Glutamine, Glutamate, and GABA in the Central Nervous System.* (Eds L Hertz, E Kvamme, EG McGeer and A Schousboe), pp. 473-492. Alan R. Liss, New York.

Hamberger, A. and Nystrom, B. (1984). Extra-and intracellular amino acids in the hippocampus during development of hepatic encephalopathy. *Neurochemistry Research,* **(9)**, 1181-1192.

Hansson, E. and Ronnback, L. (1995). Astrocytes in glutamate neurotransmission. *FASEB Journal,* **9(5)**, 343-50.

Herrera-Marshchitz, M., You, Z.B., Goiny, M., Meana, J.J., Silvereira, R., Godukhin, O.V., Chen, Y., Espinoza, S., Pettersson, E., Loidl, C.F., Lubec, G., Andersson, K., Nylander, I., Terenius, L. and Ungerstedt, U. (1996). On the origin of extracellular glutamate levels monitored in the basal ganglia of the rat by *in vivo* microdialysis. *Journal of Neurochemistry, in press.*

Hollmann, M. and Heinemann, S. (1994). Cloned glutamate receptors. *Annual Review of Neuroscience,* **(17)**, 31-108.

Hooks, M.S. and Kalivas, P.W. (1994). Involvement of dopamine and excitatory amino acid transmission in novelty-induced motor activity. *The Journal of Pharmacology and Experimental Therapeutics,* **269(3)**, 976-988.

Imperato, A., Honore, T. and Jensen, L.H. (1990). Dopamine release in the nucleus caudatus and in the nucleus accumbens is under glutamatergic control through non-NMDA receptors: a study in freely-moving rats. *Brain Research,* **530**, 223-228.

Imperato, A., Scrocco, M.G., Bacchi, S. and Angelucci, L. (1990). NMDA receptors and *in vivo* dopamine release in the nucleus accumbens and caudatus. *European Journal of Pharmacology,* **187**, 555-556.

Jacobson, I., Sandberg, M. and Hamberger, A. (1985). Mass transfer in brain dialysis devices-a new method for the estimation of extracellular amino acid concentration. *Journal of Neuroscience Methods*, **15**, 263-268.

Johnson, R.D. and Justice, J.B.J. (1983). Model studies for brain dialysis. *Brain Research Bulletin*, **10(10)**, 567-571.

Jonas, P. (1993). Glutamate receptors in the central nervous system. *Annals of the New York Academy of Science*, **707**, 126-135.

Kelley, A.E. and Throne, L.C. (1992). NMDA receptors mediate the behavioral effects of amphetamine infused into the nucleus accumbens. *Brain Research Bulletin*, **29**, 247-254.

Kita, H. and Kitai, S.T. (1990). Amygdaloid projections to the frontal cortex and the striatum in the rat. *Journal of Comparative Neurology*, **298**, 40-49.

Kitamura, T. (1980). Dynamic aspects of glial reactions in altered brains. *Pathology, Research and practice*, **168(4)**, 301-43.

Klockner, U., Storck, T., Conradt, M. and Stoffel, W. (1993). Electrogenic L-glutamate uptake in Xenopus laevis oocytes expressing a cloned rat brain L-glutamate/L-aspartate transporter (GLAST-1). *Journal of Biological Chemistry*, **268(20)**, 14594-6.

Kotake, C., Heffner, T., Vosmer, G. and Seiden, L. (1985). Determination of dopamine, norepinephrine, serotonin and their major metabolic products in rat brain by reverse-phase ion-pair high performance liquid chromatography with electrochemical detection. *Pharmacology Biochemistry Behaviour*, **22(1)**, 85-9.

Kurosawa, M., Hallstrom, A. and Ungerstedt, U. (1991). Changes in cerebral blood flow do not directly affect *in vivo* recovery of extracellular lactate through microdialysis probe. *Neuroscience Letters*, **126**, 123-126.

Laake, J.H., Slyngstad, T.A., Haug, F.M. and Ottersen, O.P. (1995). Glutamine from glial cells is essential for the maintenance of the nerve terminal pool of glutamate: immunogold evidence from hippocampal slice cultures. *Journal of Neurochemistry*, **65(2)**, 871-81.

Lerma, J., Herranz, A.S., Herreras, O., Abraira, B. and Rio, R.M.D. (1986). *In vivo* determination of extracellular concentration of amino acids in the rat hippocampus. A method based on brain dialysis and computerized analysis. *Brain Research*, **384**, 145-155.

Lindefors, N., Amberg, G. and Ungerstedt, U. (1989). Intracerebral microdialysis: I. experimental studies of diffusion kinetics. *Journal of Pharmacological Methods*, **22**, 141-156.

Lonnroth, P., Jansson, P.A. and Smith, U. (1987). A microdialysis method allowing characterization of intracellular water space in humans. *American Journal of Physiology*, **256**, E250-E255.

Lovinger, D.M. and McCool, B.A. (1995). Metabotropic glutamate receptor-mediated presynaptic depression at corticostriatal synapses involves mGLuR2 or 3. *Journal of Neurophysiology*, **73(3)**, 1076-83.

Major, O., Shdamova, T., Duffek, L. and Nagy, Z. (1990). Continuous Monitoring of Blood-Brain Barrier Opening to Cr51-EDTA by microdialysis following probe injury. *Acta Neurochirurgica, Suppl.*, **51**, 46-48.

McKenna, M.C., Sonnewald, U., Huang, X., Stevenson, J. and Zielke, H.R. (1996). Exogenous glutamate concentration regulates the metabolic fate of glutamate in astrocytes. *Journal of Neurochemistry*, **66(1)**, 386-93.

Miele, M., Berners, M., Boutelle, M.G., Kusakabe, H. and Fillenz, M. (1996). The determination of the extracellular concentration of brain glutamate using quantitative microdialysis. *Brain Research*, **708**, 131-133.

Moghaddam, B. and Bunney, B.S. (1989). Ionic composition of microdialysis perfusing solution alters the pharmacological responsiveness and basal outflow of striatal dopamine. *Journal of Neurochemistry*, **53(2)**, 652-4.

Moriyoshi, K., Masu, M., Ishii, T., Shigemoto, R., Mizuno, N. and Nakanishi, S. (1991). Molecular cloning and characterization of the rat NMDA receptor. *Nature*, **354(6348)**, 31-37.

Nicholls, D.G. (1993). The glutamatergic nerve terminal. *European Journal of Biochemistry*, **212**, 613-631.

O'Donnell, P. and Grace, A.A. (1993). Physiological and Morphological properties of accumbens core and shell neurons recorded *in vitro*. *Synapse*, **13**, 135-160.

O'Donnell, P. and Grace, A.A. (1994). Tonic D2-mediated attenuation of cortical excitation in nucleus accumbens neurons recorded *in vitro*. *Brain Research*, **634**, 105-112.

O'Donnell, P. and Grace, A.A. (1995). Synaptic interactions among excitatory afferents to nucleus accumbens neurons: hippocampal gating of prefrontal cortical input. *Journal of Neuroscience*, **15(5 Pt 1)**, 3622-39.

Osborne, P.G., O'Conner, W.T. and Ungerstedt, U. (1991). Effect of varying the ionic concentration of a microdialysis perfusate on basal striatal dopamine levels in awake rats. *Journal of Neurochemistry*, **56**, 452-456.

Pap, A. and Bradberry, C.W. (1995). Excitatory amino acid antagonists attenuate the effects of cocaine on extracellular dopamine in the nucleus accumbens. *Journal of Pharmacology and Experimental Therapeutics*, **274(1)**, 127-33.

Parsons, L.H. and Justice, J.B., Jr. (1994). Quantitative approaches to *in vivo* brain microdialysis. *Critical Reviews in Neurobiology*, **8(3)**, 189-220.

Parsons, L.H. and Justice, J.B.J. (1992). Extracellular concentration and *in vivo* recovery of dopamine in the nucleus accumbens using microdialysis. *Journal of Neurochemistry*, **58(1)**, 212-219.

Patterson, T.A., Kim, E.K., Meldrum, M.J. and Dawson, R.J. (1995). Glutamate efflux from rat brain slices and cultures: a comparison of the depolarizing agents potassium, 4-aminopyridine, and veratrine. *Neurochemical Research*, **20(2)**, 225-32.

Paulsen, R.E. and Fonnum, F. (1989). Role of glial cells for the basal and Ca2+-dependent K+-evoked release of transmitter amino acids investigated by microdialysis. *Journal of Neurochemistry*, **52(6)**, 1823-1829.

Pin, J.P. and Duvoisin, R. (1995). The metabotropic glutamate receptors: structure and functions. *Neuropharmacology*, **34(1)**, 1-26.

Pulvirenti, L., Swerdlow, N.R. and Koob, G.F. (1991). Nucleus accumbens NMDA antagonist decreases locomotor activity produced by cocaine, heroin or accumbens dopamine, but not caffeine. *Pharmacology Biochemistry and Behaviour*, **40**, 841-845.

Robinson, T.E. and Camp, D.M. (1991). The effects of four days of continuous striatal microdialysis on indices of dopamine and serotonin neurotransmission in rats. *Journal of Neuroscience Methods*, **40(2-3)**, 211-222.

Robinson, T.E. and Camp, D.M. (1992). On the use of multiple probe insertions at the same site for repeated intracerebral microdialysis experiments in the nigrostriatal dopamine system of rats. *Journal of Neurochemisty*, **58(5)**, 1706-1715.

Sakimura, K., Bujo, H., Kushiya, E., Araki, K., Yamazaki, M., Meguro, H., Warashina, A., Numa, S. and Mishina, M. (1990). Functional expression from cloned cDNAs of glutamate receptor species responsive to kainate and quisqualate. *FEBS Lett.*, **(1-2)**, 73-80.

Sam, P.M. and Justice, J.B.J. (1996). Effect of general microdialysis-induced depletion on extracellular dopamine. *Journal of Neurochemistry*, **in press**,

Schultz, W., Apicella, P., Scarnati, E. and Ljungberg, T. (1992). Neuronal activity in monkey ventral striatum related to the expectation of reward. *Journal of Neuroscience*, **12**, 4595-4610.

Sekiguchi, M., Wada, K. and Wenthold, R.J. (1992). N-acetylaspartylglutamate acts as an agonist upon homomeric NMDA receptor (NMDAR 1) expressed in Xenopus oocytes. *FEBS Lett.*, **311**, 285-289.

Sesack, S.R., Deutch, A.Y., Roth, R.H. and Bunney, B.S. (1989). Topographic organization of the efferent projections of the medial prefrontal cortex in the rat: an anterograde tract-tracing study using *Phaseolus vulgaris* leucoagglutinin. *Journal of Comparative Neurology*, **290**, 213-242.

Shuaib, A., Xu, K., Crain, B., Sirren, A.L., Feuerstein, G., Hallenbeck, J. and Davis, J.N. (1990). Assessment of damage from implantation of microdialysis probes in the rat hippocampus with silver degeneration staining. *Neuroscience Letters*, **112**, 149-154.

Stein, E., Cox, J., A., Seeburg, P.H. and Verdoorn, T.A. (1992). Complex pharmacological properties of recombinant alpha-amino-3-hydroxy-5-methyl-4-isoxazole propionate receptor subtypes. *Molecular Pharmacology*, **13**, 864-871.

Sternson, L.A., Stobauch, J.F. and Repta, A.J. (1985). Rational design and evaluation of improved 0-phthaladehyde-like fluorogenic reagents. *Analytical Biochemistry*, **144**, 233-246.

Szatkowski, M., Barbour, B. and Attwell, D. (1990). Non-vesicular release of glutamate from glial cells by reversed electrogenic glutamate uptake. *Nature*, **348**, 443-445.

Taber, M.T. and Fibiger, H.C. (1995). Electrical stimulation of the prefrontal cortex increases dopamine release in the nucleus accumbens of the rat: modulation by metabotropic glutamate receptors. *Journal of Neuroscience*, **15(5 Pt 2)**, 3896-904.

Tossman, D. and Ungerstedt, U. (1986). Microdialysis in the study of extracellular levels of amino acids in the rat brain. *Acta Physiology Scandanavia*, **124**, 9-14.

Totterdell, S. and Smith, A.D. (1989). Convergence of hippocampal and dopaminergic input onto identified neurons in the nucleus accumbens of the rat. *Journal of Chemical Neuroanatomy*, **2(5)**, 285-98.

Ungerstedt, U. (1984). Measurement of neurotransmitter release by intracranial dialysis. in measurement of neurotransmitter *in vivo*. New York, John Wiley and Sons.

Wages, S.A., Church, W.H. and Justice, J.B., Jr. (1986). Sampling considerations for on-line microbore liquid chromatography of brain dialysis. *Analytical Chemistry*, **58**, 1649-1656.

Wang, J., Lieberman, D., Tabubo, H., Finberg, J.P., Oldfield, E.H. and Bankiewicz, K.S. (1994). Effects of gliosis on dopamine metabolism in rat striatum. *Brain Research*, **663(2)**, 199-205.

Westerink, B.H.C. and DeVries, J.B. (1988). Characterization of *in vivo* dopamine release as determined by brain microdialysis after acute and subchronic implantations: methodological aspects. *Journal of Neurochemistry*, **51(3)**, 683-687.

Westerink, B.H.C., Hofsteed, H.M., Tuntler, J. and DeVries, J.B. (1989). Use of calcium antagonism for the characterization of drug-evoked dopamine release from the brain of conscious rats determined by microdialysis. *Journal of Neurochemistry*, **52**, 722-729.

Wise, R.A., Fotuhi, M. and Colle, L. (1989). Facilitation of feeding by nucleus accumbens amphetamine: Latency and speed measures. *Pharmacology Biochemistry and Behavior*, **32**, 769-772.

Woodroofe, M.N., Sarna, G.S., Wadhwa, M., Hayes, G.M., Loughlin, A.J., Tinker, A. and Cuzner, M.L. (1991). Detection of interleukin-1 and interleukin-6, in adult rat brain, following mechanical injury, by *in vivo* microdialysis: evidence of a role for microglia in cytokine production. *Journal of Neuroimmunology*, **33(3)**, 227-236.

Wu, M., Brudzynski, S.M. and Mogenson, G.J. (1993). Functional interaction of dopamine and glutamate in the nucleus accumbens in the regulation of locomotion. *Canadian Journal of Physiology and Pharmacology*, **71(5-6)**, 407-13.

Yang, C.R. and Mogenson, G.J. (1984). Electrophysiological responses of neurones in the nucleus accumbens to hippocampal stimulation and the attenuation of the excitatory responses by the mesolimbic dopaminergic system. *Brain Research,* **324(324),** 69-84.

Yang, C.R. and Mogenson, G.J. (1986). Dopamine enhances terminal excitability of hippocampal-accumben neurons via D2 receptor: role of dopamine in presynaptic inhibition. *Journal of Neuroscience,* **6(8),** 2470-8.

Yergey, J.A. and Heyes, M.P. (1990). Brain eicosanoid formation following acute penetration injury as studies with brain microdialysis. *Journal of Cerebral Blood Flow and Metabolism,* **10(1),** 143-146.

Yim, C.Y. and Mogenson, G.J. (1986). Mesolimbic dopamine projection modulates amygdala-evoked EPSP in nucleus accumbens neurons: an *in vivo* study. *Brain Research,* **369(1-2),** 347-52.

Youngren, K.D., Daly, D.A. and Moghaddam, B. (1993). Distinct actions of endogenous excitatory amino acids on the outflow of dopamine in the nucleus accumbens. *Journal of Neurochemistry,* **5,** 1650-1657.

Zetterstrom, T., Sharp, T., Marsden, C.A. and Ungerstedt, U. (1983). *In vivo* measurement of dopamine and its metabolites by intracerebral dialysis: Changes after d-amphetamine. *Journal of Neurochemistry,* **41,** 1769-1773.